Reviewer 2:

The author describes an approach for a detection method for avalanches based on hidden Markov models, applied on a seismic array. I' am wondering about the high computational and installation effort (two arrays) needed for this detection method, which does not make sense for practical applications. Also the false alarm ratio is relatively high, although a complicated detection method is used. However, the method and the results are well presented and the work has a scientific relevance for seismic signal processing , so I recommend to accept this article with minor revision:

Page 1, line 11: "small changes of source direction" - this depends on the location array - avalanche path
This is correct. However, since our array is located at the valley bottom, we expect only small changes for the back-azimuth. We clarified it in the abstract.
Since snow avalanches recorded at our arrays typically generate signals with small changes in source direction, events with large changes were dismissed as false detections.

Page 2, line 13-18: Might mention that infrasound detection methods for avalanches currently shows better results than seismic detection. Of course this depends on the avalanche type, so powder avalanches produce higher infrasound amplitudes, while wet snow avalanches generate higher seismic signals. You can also notice, that a combination of both technologies might result in a better detection performance.
We added a few sentences in the introduction to address this issue.
A recent comprehensive study on the performance of these systems has shown that in the absence of major topographic barriers, infrasound avalanche detection systems relying on array processing techniques are well suited to reliably monitor larger avalanches up to a distance of 3 to 4 kilometers (Mayer et al. 2018).

Page 3, line 10: "natural frequency" instead of "eigenfrequency"
We changed the term.

Page 4, sec. 3.1: What does this threshold mean for the possible detectable avalanche size? Have you thought about using the common STL/LTA method?
This threshold was only used to reduce the amount of data to process. It is similar to the STA/LTA method, however, since we are not interested in the exact onset of seismic signals (which is a big advantage of the STA/LTA method, especially for earthquake detection), a much simpler amplitude threshold was sufficient.

Page 7, line 25: I'm wondering, that you can find one representative avalanche event for training, which can be used for the whole winter season. Normally there a large differences at the signal pattern for different avalanche types (powder to wet snow avalanches).
In previous studies, we investigated using different avalanche signals to represent different classes (i.e. dry and wet-snow avalanches). However, this approach did not improve the classification results. Signals from different types of avalanches have some distinct characteristics: wet-snow avalanches generally generate longer signals (these avalanches flow more slowly) and higher amplitudes (larger mass often flowing on the bare ground). Nevertheless, when using HMMs for the classification, the duration of the signal and the maximum amplitude are not relevant and there is no need to implement specific avalanche classes.

Page 8, line 8: Is not it theoretical possible that an avalanche occur right between this two arrays and is than registered by both?
The maximum distance for an avalanche to be detected is around 3 km. Since both arrays are seperated by about 14km, avalanches occurring right between those arrays are likely not detected at all. Furthermore, it is possible that avalanches releases simultaneously at both array. However, we assume this probability to be rather low.

Page 9, line 20-24: What does this minimum event duration mean for detectable avalanche sizes?
It is clear that imposing a duration threshold for the detections does not allow us to investigate small avalanches. However, due to a lack of ground truth data, we did not investigated the influence of avalanches size. Previous work has shown that signal duration relates to avalanche size. However, as powder avalanches travel at higher velocities than wet snow avalanches, a long duration of the signal might indicate a large and fast powder avalanche with a long runout, or a slow wet snow avalanche with a shorter runout and size. Thus, we cannot comment specifically on what avalanche size is excluded due to our minimum duration threshold.

Sec. 5: A graphic comparing the number of detected avalanches, false alarms (maybe separated for every detection criterion) and also the number of missed events for the whole season would be useful. Especially I missed a detailed description about the missed events.
We included an additional Table containing these numbers.

Page 20, line 10: Might you can also note literature about seismic detection of debris flow/debris flood - this are sometimes similar to the detection methods for avalanches.
We have added more references in the Discussion section related to other types of gravitational mass movements.

Page 21, line 12: Efficient for your situation, but the need of two different arrays is not a "efficient approach".
We now address this point in the Discussion section:
Our suggested workflow requires two arrays to eliminate falsely classified events by finding co-detections. This is clearly a limiting factor as it increases the cost for the instrumentation as well as deployment and maintenance time.

Review of
Automatic detection of avalanches using a combined array classification and localization
by Heck et al.

1st Revision

The two reviewers of the original submission pointed out several specific issues within the manuscript. The authors responded to all of these comments, yet sometimes it is hard for me to check if or how those replies made it into the revised version of the manuscript. Additionally I think the manuscript still needs work before it can be accepted for publication. Please find my detailed comments below.

Best regards,
Florian Fuchs

Handling of reviewer comments:

The authors reply properly to all reviewer comments. However, especially when answering to Reviewer #1 comments on pages 12 and later it's not clear anymore if those replies were integrated into the manuscript. I do support all of the reviewers comments and questions and I do see that the authors know how to respond to those. But I strongly suggest to implement all of them – at least briefly – into the manuscript. The same holds for almost all comments by Reviewer #2.
Please insert all of those replies to the text (at least briefly) and indicate all the changes in the rebuttal letter. Otherwise, it's hard to follow, not having done the 1 st round of reviews.

Additional comments:
Although all/many comments from the first round of reviews were already taken care of, I must unfortunately admit that I still had a hard time reading the manuscript. I do believe that work itself is interesting and the findings are worth reporting. Yet, the manuscript is not easily comprehensible in the current shape. Mainly, I am missing a clear and concise structure and more precision in the wording and figures. I also suggest to make use of the Copernicus English grammar and spellchecking service.

We would like to thank the reviewer for the helpful comments. Based on these comments, we substantially changed the manuscript to improve the structure and clarity of the text. We have also (briefly) included many of our replies of the first round of reviews in the discussion.

General structure and ease of reading:

- Please be more precise throughout the entire manuscript. When you say "high", "low", "good", "poor", "better", "most", "large" please try to give values, if possible. E.g., what number of percentage can be considered a "good" classification result? When you speak of "features" that "change" and are "common" please describe specifically which features you mean and how they change.

We checked the manuscript and changed the wording in places where it was ambiguous.

- Your chain of processing kind of gets obscured throughout the manuscript. I'd suggest that somewhere you briefly list your work flow. Figure 5 somewhat tries to summarize this, but I think text would help here. Additionally, Figure 5 could use some instructive labels, e.g. you could indicated the length of the data windows. The panels "pre-processing" and

especially “post-processing” could indicate what’s actually done. E.g. that post-processing is the MUSIC beamforming.

We completely restructured the methods and results sections to more clearly convey how the suggested signal processing workflow works.

- I am missing a short subsection on “post-processing” in section 3, “methods”. You repeatedly emphasize the need for “post-processing” but it’s not clear what this is.

We added a section to more clearly explain the different stages in the post-processing.

- In principle it is a good idea to have dedicated sessions on methods and results (sections 3 and 4 in this manuscript). Yet, you mix methods, observations, interpretation and references repeatedly. In the “Methods” section you should be as brief and precise and necessary. You should not evaluate the results of other work here, but only briefly repeat the main points you make use of. All the rest is better placed in the discussion section. Likewise, in the results section (4) you repeatedly evaluate the quality of the results (this should be done in the discussion section) or introduce new steps in the processing. Please double-check to clarify.

As mentioned before, we completely restructured the methods and results sections. Furthermore, we moved some sections of the text to either the introduction or the discussion.

- It’s difficult to track how many events you remove during the different processing steps and how many events actually remain as final detections. Maybe a table listing the number of events and how many get discarded by each processing step would help.

We added an additional table showing the number of detection and false classification for each processing step.

Discussion section:

- I agree with Reviewer #1 that the “Discussion” section in the current state is rather a repetition and summary of the previous chapters. This needs to be changed. Here I’d like to see you discuss the benefits and limitations of your methods. E.g. it is very interesting to read that the sensor installation itself already has a huge impact on the classification results. Why? What else can influence the classification that strongly? The airplane signal could also be discussed here (or in the supplemental, see below), as reviewer #2 points out the strong difference to other observed airplane signals. What about anthropogenic signals? Are there roads/cars nearby?

We rewrote most of the Discussions section and now also explicitly address the airplane signals that were falsely classified as avalanches.

- Most importantly, the choice of the training event should be discussed, as it surely has a huge impact. For example why did you only choose a part of the avalanche signal in Figure 7 as the training event? Half of the signal seems to be missing ... You may not have the time and patience now to carefully double-check the performance of your routine based on different training events, but this would of course be desirable. Do you maybe at least have some experience from other datasets that you can report on? Why can’t you simply use more than one training event?

As mentioned in the discussion section now, it was best to neglect the coda of the avalanche signal and only use the part of the signal where energy increases up to the first maximum of the signal. We also investigated using different sections of the avalanche signal without improving the classification results. In the past, we have investigated using different training events for dry- and wet-snow avalanches to improve our classification results. However, such an approach did not improve the results at all and typically resulted in more falsely classified events. While we did not conduct a comprehensive investigation on the influence of the training event, our ad-hoc testing has

shown that the influence is rather limited. Furthermore, we also wanted to highlight that it is possible to use this classification approach with only one training event.

- Could you think of other "features" that could help to distinguish avalanches from airplanes and earthquakes? After all, the ones you use don't seem to do the job. I'd personally like to see you speculating here …

We investigated using other and more features in our recent work (Heck et al. (2018)). In the end, the feature combination used for the classification in the current work was the best suitable for the classification task.

- Obviously, broadband sensors will not necessarily improve your data quality, neither will they automatically detect more distant avalanches. This needs to be rephrased. Only in the rare case of huge, catastrophic events – which generate long period seismic radiation, in contrast to the small local ones – they might be an advantage over the short-period geophones. The fact that "common" avalanches can only be detected within few km distance is probably due to the weak seismic signal they generate, and the only chance to improve the data quality is to have more sensors (signal-to-noise ratio) closer to the events (less attenuation). Of course, this is not always possible.

We agree with the reviewer that changing the instrumentation is not likely going to improve the data quality nor the detection range. We therefore removed this section.

Efficiency of computations:

- When discussing the "speed of processing" you refer to a "standard 8 core processor with 16GB RAM". It may seem picky now, but do you actually make use of all the 8 cores? Is there some kind of parallelization involved in your processing? If yes, please comment on this, if not I think the community usually refers to "a standard personal desktop/laptop computer" to indicate that no supercomputing powers or high-level workstations are required. Similarly, do you actually need the 16GB RAM? If yes, what for? Reviewer #2 also pointed this out and it's actually an interesting point. In fact, probably the computing power wouldn't really matter and you would not have to comment on it, if data were only processed "off-field" in some data center. However, In your reply, you indicate that some of the processing is done on-site in the field – this of course strongly limits computational power and is a very interesting and crucial point that is not mentioned at all in the manuscript. Please include this in the Instrumentation/Methods section! This will also clarify why you perform some of the processing steps and why computation time is crucial.

We did not perform an in-depth analysis of our computing time, nor did we try to optimize our algorithms for this. We only wanted to comment on this to show that the method could be used in near real-time and that the most costly analysis is the MUSIC method. We do not perform any processing on-site in the field, this must be a misunderstanding or some unclear comments in our earlier replies. Note that it is useful to have a multicore processor, since several tasks can be performed simultaneously (e.g. computing the features of all seven sensors at the same time). We now only very briefly comment on this at the end of the Discussion section.

Figures:

- There are a lot of Figures, which complicates the reading. I suggest to e.g. somehow merge Figures 6, 8, 12 and 14 as they all show the same information. If all the panels were shown below each other, a comparison of the observations would be easier.
- Similarly, maybe Figures 2 and 3 could be merged.

We merged and improved some of the figures

- Please highlight the avalanches in Figure 4.

We highlighted avalanches in this figure and also included the location of the cameras and the seismic array.

- Figures 9 + 11 are not relevant for the understanding of the text and I suggest to move those to the supplemental material. Reviewer #2 raised doubts about the origin of the airplane signals, since they look different in other studies. The authors claim to be certain about their interpretation. This point might also be discussed in the supplemental material, as it's not crucial for the understanding of the main text.

We do not agree with the reviewer that these figures are not relevant. In our opinion these figures clearly show the two main types of signals that were falsely classified. Furthermore, one can clearly see that the signals recorded at both arrays are very similar. This is particularly important for our airplane signals, which do not contain any signs of Doppler effect or clear overtones and are therefore rather unusual. We therefore kept these figures in the main text, but we merged them into one figure.

Automatic detection of avalanches using a combined array classification and localization

Matthias Heck[1], Alec van Herwijnen[1], Conny Hammer[2], Manuel Hobiger[2], Jürg Schweizer[1], and Donat Fäh[2]

[1]WSL Institute for Snow and Avalanche Research SLF, Davos
[2]Swiss Seismological Service SED, ETH Zurich, Zurich

Correspondence: Matthias Heck (matthias.heck@slf.ch)

Abstract.

We used ~~continuous data from~~ a seismic monitoring system to automatically determine the avalanche activity at a remote field site ~~above~~ near Davos, Switzerland. ~~The approach is based on combining a machine learning algorithm with array processing techniques to provide an operational method capable of near real-time classification. First, we used~~ By using a recently developed ~~method~~ approach based on hidden ~~Markos~~ Markov models (HMMs), a machine learning algorithm, we were able to automatically identify ~~events~~ avalanches in continuous seismic data by ~~using only~~ providing a single training event. Furthermore, we implemented an operational method to provide near real-time classification results. For the 2016-2017 winter period ~~, this resulted in~~ 117 events ~~. Second, to eliminate falsely~~ were then automatically identified. False classified events such as airplanes and local earthquakes were filtered using a new approach containing two additional classification steps. In a first step, we implemented ~~an additional~~ a second HMM based classifier at a second array $14\,\mathrm{km}$ away to automatically identify airplanes and earthquakes. By cross-checking the results of both arrays ~~,~~ we reduced the number of false classifications by about $50\,\%$. In a ~~third and final step~~second step, we used multiple signal classifications (MUSIC), an array processing technique, to determine the direction of the source. ~~Since snow avalanches recorded at our arrays typically generate signals with small changes in source direction , events with large changes were dismissed as false detections~~Although avalanche events have a moving source character, only small changes of the source direction are common whereas false classifications showed large changes and thus were dismissed. From the 117 initially detected events during the 4-month period ~~, our classification workflow removed 96 events as false classifications . The majority of the remaining 21 events were on 9 and 10 March 2017,~~ we were able to identify 90 false classifications based on these two additional steps. The avalanche activity based on the remaining 27 avalanche events was in line with visual ~~avalanche observations~~ observations performed in the region of Davos. ~~Our results suggest that the presented classification workflow could be used to identify major avalanche periods and highlight the importance of array processing techniques for the automatic classification of avalanches in seismic data.~~

1 Introduction

During the winter seasons, snow avalanches are a common threat in ~~mountainous~~ mountain regions. Avalanche warning services therefore inform the public of the current avalanche danger. To assess the danger, warning services rely on information about the snowpack, amount of new snow, weather conditions and avalanche activity ~~(e.g. McClung and Schaerer, 2006)~~(McClung and Sch
Whereas the first three parameters can be measured or modeled, avalanche activity data are often hard to obtain, especially during snow storms or at night. Monitoring systems ~~can possibly fill this gap by providing information on avalanche activity independent of the time of day or visibility~~have therefore been developed to estimate the avalanche activity for a certain region.

Snow avalanches, like any other mass movement, generate seismic and infrasound waves (e.g. van Herwijnen and Schweizer, 2011b; Suriñach et al., 2005; Marchetti et al., 2015). Seismic signals of avalanches show some common characteristics, including a spindle shaped envelope of the time series (Nishimura and Izumi, 1997) and a typical frequency content between 2 and 30 Hz (Schaerer and Salway, 1980; Suriñach et al., 2001). Several classification approaches were therefore developed to automatically detect avalanches in seismic data. Leprettre et al. (1996) used a fuzzy logic approach to distinguish between different types of signals. Bessason et al. (2007) ~~applied~~ used a nearest neighbor approach ~~and detected~~ to classify new recorded events. Using this approach, they were able to detect 65 % of all confirmed avalanches. Rubin et al. (2012) compared 12 machine learning algorithms, 10 of which were able to detect at least 90 % of all manually identified avalanches~~. While these machine learning methods perform reasonably well in terms of detecting confirmed avalanche events, a large training data set is typically required and~~ , however, at the cost of very high false alarm rates~~are generally rather high (Rubin et al., 2012).~~

~~An alternative machine learning approach was recently presented by Hammer et al. (2017) . They~~ . Hammer et al. (2017) recently used hidden Markov models (HMMs), an advanced machine learning algorithm, to automatically detect large avalanches released ~~in February 1999~~ during the winter of 1998-1999 in seismic data recorded by a single broadband station maintained by the Swiss Seismological Service (SED). ~~HMMs use a sequence of multivariate Gaussian probability distributions to model observations (e.g. seismic time series). To determine the characteristics of the distributions (i.e. mean and covariance), classical HMMs also require a large number of training sets for each event class (e.g. avalanche, airplane or earthquake). This classical approach was successfully used to automatic identify seismic events in continuous seismic data (Ohrnberger, 2001; Beyreuther et al., 2012). Avalanches, however, are relatively rare events and obtaining a large set of training events is time consuming. To circumvent this, Hammer et al. (2012) developed an approach exploiting the abundance of data containing mainly background signals to obtain general wave-field properties. From these properties, a widespread background model was learned and only one training event was required. In contrast to the classical HMM approach, the classification system thus consists of a background model and one event model for each implemented event class.~~ Using this approach, ~~Hammer et al. (2017)~~ they were able to identify 43 ~~destructive avalanches during an exceptional~~ avalanches during a 5-day ~~avalanche period in February 1999~~ period within a radius of 30 km of the ~~broadband seismic~~ station. Heck et al. (2018a) ~~recently adapted this~~ also used the HMM approach to automatically detect ~~smaller avalanches~~avalanches, however, in data recorded during the winter season 2009-2010 by a seismic array consisting of seven less sensitive vertical geophones~~during the winter season 2009-2010. Despite the large differences in model performance for the individual sensors, their model performed best when pooling the data from the entire array~~ .

They obtained the best results for the automatic detection by combining the classification results of all sensors and requiring a minimal event duration for the detections. ~~These results highlighted that array based processing is likely to improve~~

Apart from using seismic signals for the automatic detection of avalanches~~in continuous seismic data.~~

~~Array processing techniques have been used to exploit infrasound signals for the automatic detection of avalanches~~ , several studies focused on the use of infrasound signals. Localization parameters determined using cross-correlation techniques were used to automatically identify avalanches in continuous data sets (Scott et al., 2007; Marchetti et al., 2015; Thüring et al., 2015). By comparing the back-azimuth with the directions of known avalanche paths, possible avalanche events were identified (Marchetti et al., 2015). Thüring et al. (2015) used a similar approach for the automatic detection, but relied on support vector machines (SVM), a machine learning algorithm. ~~The success of array processing techniques on infrasound signals led to the development of operational avalanche detection systems to automatically identify avalanches (Steinkogler et al., 2016). A recent comprehensive study on the performance of these systems has shown that in the absence of major topographic barriers, infrasound avalanche detection systems relying on~~

In addition to the automatic detection of avalanches, Lacroix et al. (2012) and Heck et al. (2018b) used seismic array processing techniques ~~are well suited to reliably monitor larger avalanches up to a distance of 3 to 4 kilometers (?).~~

~~Array processing techniques have also been used~~ to locate the source of ~~avalanches in seismic data~~the avalanche. Lacroix et al. (2012) implemented a beam-forming approach and were able to assign recorded avalanches to three known avalanche paths. Heck et al. (2018b) compared a beam-forming method with a multiple signal classification (MUSIC) approach (Schmidt, 1986) and obtained better results with the latter ~~. The MUSIC method is based on the covariance matrix of all sensors, whereas beam-forming methods rely on pair-wise cross-correlation (Schmidt, 1986; Rost and Thomas, 2002). Heck et al. (2018b)~~ and they subsequently applied this method to ~~manually identified avalanches~~ avalanches monitored during a two-day period in March ~~2017 and were able to reconstruct the avalanche path of several recorded events. They~~ 2017. Based on these results they concluded that their seismic array mostly recorded infrasound ~~signals~~ due to the limited distance between the sensors. ~~While both~~ Nevertheless, they were able to reconstruct the avalanche path of several recorded events. Lacroix et al. (2012) and Heck et al. (2018b) ~~showed that avalanches within a distance of approximately~~ both used less sensitive vertical component geophones for the seismic monitoring resulting in an avalanche detection distance of approximately 3 km~~of their seismic monitoring systems were detected, seismic array processing techniques have not yet been used for the automatic detection of avalanches in seismic data~~.

Our aim is to ~~design a workflow to~~ automatically identify avalanches in continuous ~~seismic data . Our method consists of using the~~ data recorded during the winter period 2016-2017 using the same machine learning techniques based on hidden Markov models ~~presented by Heck et al. (2018a)in combination with seismic array processing techniques to locate the source of avalanches presented by Heck et al. (2018b) . The goal is to assess the performance of a fully automatic classifier in view of possible future operational use. To develop and test the automatic classification method, we used continuous seismic data recorded~~ as used by Heck et al. (2018a). To reduce the false alarm rate we first use an additional classification performed at a second array 14 km away to dismiss events recorded almost simultaneously at both arrays such as earthquakes and airplanes. In a second step, we analyze the median back-azimuth path of the detections using the MUSIC method as performed by

Heck et al. (2018b) and dismiss all events with a randomly distributed back-azimuth. We performed the classification and localization of the events with the data recorded at the seismic array located in the Dischma Valley above Davos, Switzerland during the winter season 2016-2017 ~~at two field sites above Davos, Switzerland~~(yellow square in Figure 1). These results were then combined with data obtained at the Wannengrat array, which is located 14 km to the northwest of the Dischma field site (red square in Figure 1).

2 Field site and instrumentation

~~During~~ Prior to the 2016-2017 winter season, we installed two seismic arrays above Davos, Switzerland~~(Figure 2). The arrays were~~ , similar to the ~~system~~ systems described by van Herwijnen and Schweizer (2011a). The first array was deployed at the Dischma field site (yellow square in Figure ~~2~~1), 14 km away from Davos at the end of a tributary valley (Heck et al., 2018b). The field site is a flat meadow at an elevation of 2000 m a.s.l. surrounded by mountain peaks which rise up to 3000 m. The second array was deployed at the Wannengrat field site above Davos at ~~2400 m~~ 2500 m a.s.l. (red square in Figure ~~2~~1). This field site is surrounded by several avalanche starting zones (van Herwijnen and Schweizer, 2011a).

Both arrays consisted of a 300 m long string with 7 vertical component geophones with an ~~natural frequency~~ eigenfrequency of 4.5 Hz. The sensors of the Dischma array were buried ~~about~~ 50 cm deep into the ground whereas the sensors at the Wannengrat field site were attached to rocks using an anchor. For each array ~~,~~ the sensors were circularly arranged (Figure 2 a) and b). The maximum distance between two sensors at the Dischma and Wannengrat field site was 64 m and 74 m, respectively, and the average distance was 36 m at the Dischma array and 45 m ~~, respectively~~at the Wannengrat array.

The instrumentation and data logging systems were identical for both arrays. Data were continuously ~~recorded at a sampling~~ sampled at a rate of 500 Hz. ~~Due~~ However, due to technical problems ~~,~~ only two sensors of the Wannengrat array recorded data throughout the entire winter (4 and 5 in Figure 2 b)~~and no data were collected between 12 and 20 January 2017. .~~ Both field sites were ~~also~~ equipped with several automatic weather stations (3 at Dischma, 4 at Wannengrat) as well as automatic cameras (8 at Dischma, ~~6~~ 5 at Wannengrat)~~to monitor~~ . The automatic cameras visually monitored the surrounding slopes ~~. Images~~ and images were recorded every 10 minutes throughout the winter (Figure 3). ~~In addition~~As already shown for avalanche activity periods in the winter season 2009-2010 by van Herwijnen and Schweizer (2011b), those images can help to identify and confirm seismic events produced by avalanches. In addition to the automatic cameras, we also performed ~~a field survey at the Dischma site on 15 March 2017~~ field surveys shortly after a period of high avalanche activity to identify avalanches and map their outlines (Figure 4) (Heck et al., 2018b).

3 Methods

~~The overall goal was to develop a processing workflow to automatically identify avalanches in seismic data from the Dischma field site by combining HMMs with seismic array processing techniques. The developed workflow consists of five steps~~

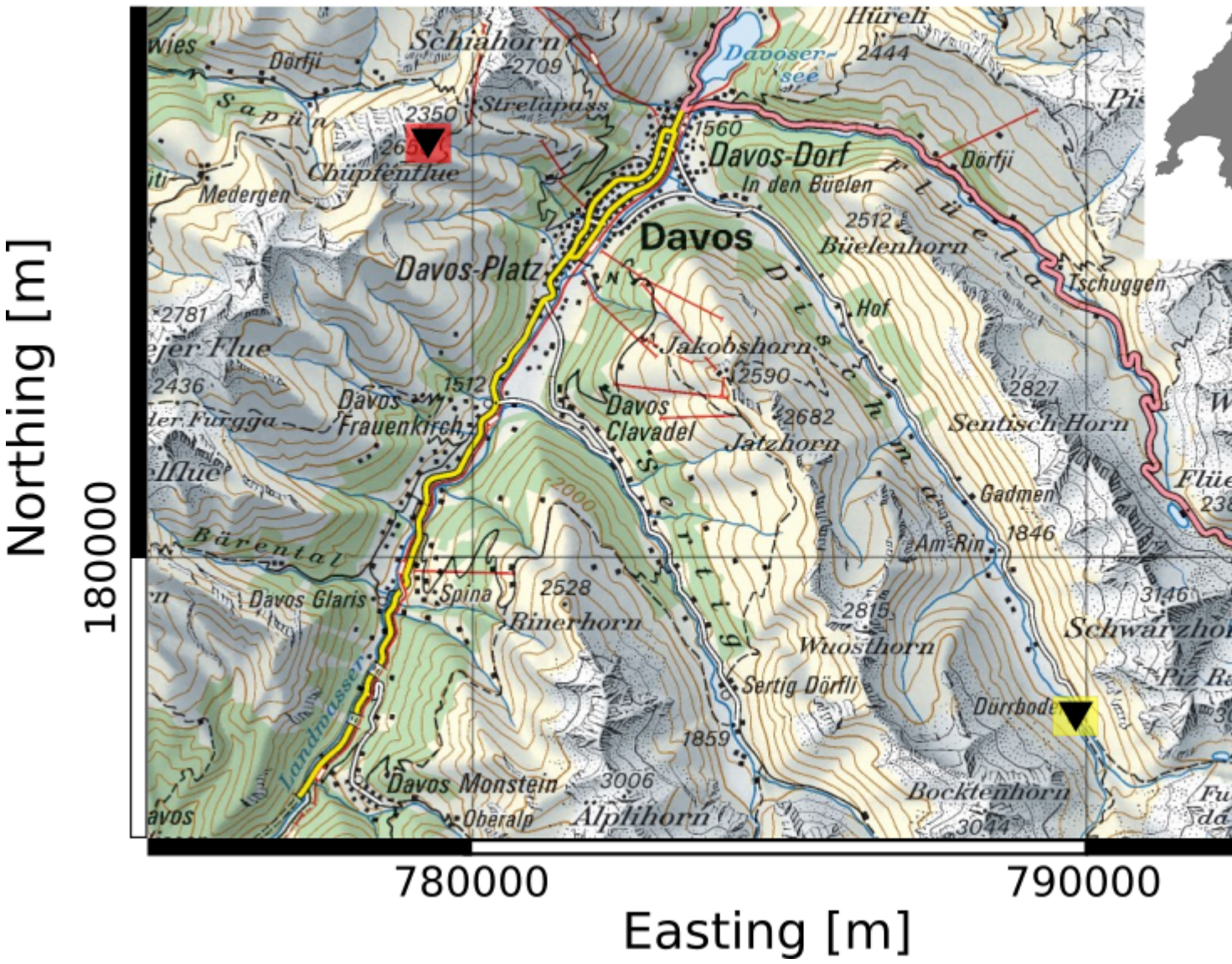

Figure 1. Map of the area of Davos, Switzerland. The two arrays are indicated by a black triangle on colored ground. Red represents the Wannengrat array, yellow the Dischma array. Reproduced by permission of swisstopo (JA100118).

(~~b~~a)

(~~a~~)

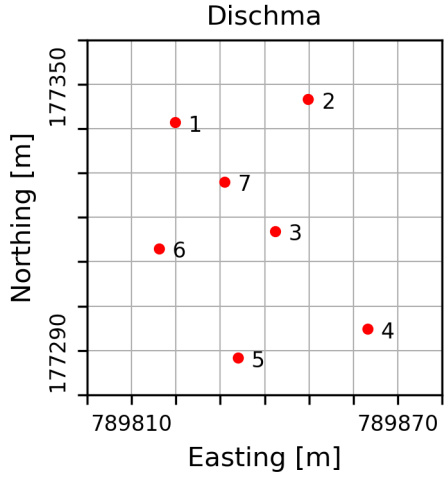

(~~c~~b)

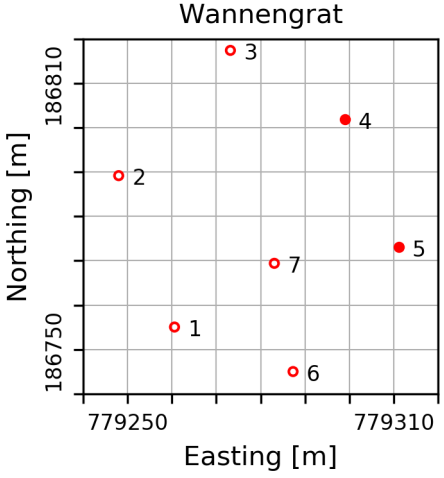

Figure 2. ~~a) Map of the area~~ Setup of ~~Davos, Switzerland. The two seismic~~ sensor arrays ~~are indicated by a black triangle on colored background. Red represents the Wannengrat array, yellow the Dischma array. The wind wheel indicates the location of the Weissfluhjoch weather station. (b) Deployment geometry of the~~ Dischma~~array. (c~~, b) ~~Deployment geometry of the~~ Wannengrat~~array~~. The open red circles indicate positions of ~~malfunctioning~~ not working sensors during the winter 2017.~~Reproduced by permission of swisstopo (JA100118).~~

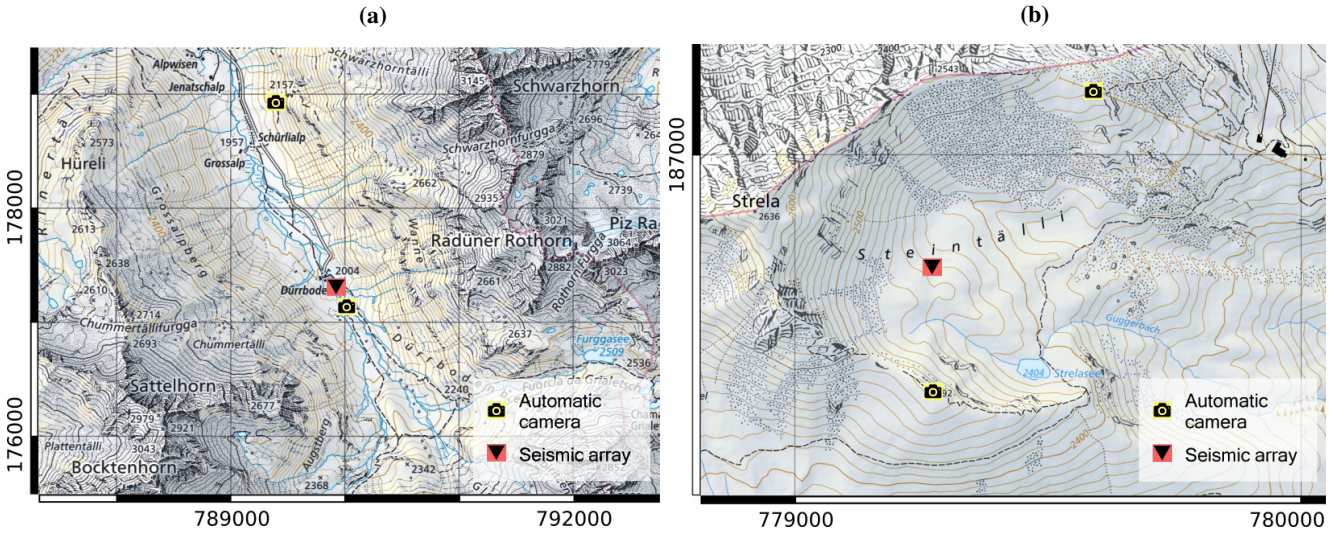

Figure 3. ~~(a)~~ Detailed map of the ~~Dischma~~ field ~~site showing~~ sites a) Dischma, b) Wannengrat. On the ~~position~~ map the positions of the seismic ~~array and~~ sensors, automatic cameras and weather stations are indicated. ~~(b) Same for~~ Due to scaling not every weather station is shown on the ~~Wannengrat field site~~map.

~~which are described in more detail below (Figure 5): (1) pre-processing, (2) feature calculation, (3) HMM construction, (4) classification and (5) post-processing.~~

~~Flow chart of the classification process. Green lines show the construction of the event model. Blue lines show the construction of the background model. The orange lines show, how the data to be classified are processed.~~

3.1 Data pre-processing

The continuous seismic data mostly ~~consisted of noise, which~~ consist of noise. Since for the current application ~~was~~ noise is of little interest~~. We therefore~~ , we applied a simple threshold based event detector to reduce the ~~total~~ amount of data (Heck et al., 2018a). For a window i with a length of 1024 samples ~~, we determined the~~ a mean absolute amplitude A_i was determined. When $A_i \geq 5\overline{A}$, with $\overline{A}$ the daily mean amplitude, the data within the window were ~~kept~~cut. If the amplitude threshold for the following window was also reached, data were concatenated. Furthermore, a section of $t = 60\,\mathrm{s}$ was cut before and after the ~~threshold passing were kept~~ window to ensure that the onset and coda of ~~events were~~ each event was incorporated. Doing so, data were reduced by $80\,\%$ to several data windows of various lengths. In addition, we filtered the data using a 4th order Butterworth bandpass filter with corner frequencies of 1 and $50\,\mathrm{Hz}$.

3.2 ~~Feature calculation~~Classification of events

~~Raw~~ To automatically identify avalanches in the continuous seismic data we used hidden Markov models (HMMs) (Rabiner, 1989). These statistical classifiers use a sequence of multivariate Gaussian probability distributions to model observations (e.g. seismic time series~~are not suited for the HMM classification, as information which characterizes seismic signals generated by~~

Figure 4. Picture of the field site of Dischma facing to the south. It was taken on 15 March 2017 shortly after a period of high avalanche activity and several recent avalanches were observed~~(red areas). The triangle indicates the location of the seismic array and the camera icon the location of the automatic camera~~.

~~avalanches in the time and frequency domain cannot be exploited. We therefore used specific features of~~). To determine the characteristics of the distributions (i.e. mean and covariance) a large number of training sets of known events, so called pre-labeled training sets, are required. For each different type of observation (e.g. avalanche, airplane or earthquake in the seismic data) a separate HMM is trained. By combining all HMMs the whole classification system with several classes is constructed. This classical approach, which relies on a large number of well-known pre-labeled training sets, was successfully used to automatic identify seismic events in continuous seismic data (Ohrnberger, 2001; Beyreuther et al., 2012). Avalanches, however, are rare events and it is nearly impossible and too time consuming to obtain a large training set. To circumvent this, we performed the classification based on an approach developed by Hammer et al. (2012) exploiting the abundance of data containing mainly background signals to obtain general wave-field properties. From these properties a widespread background model can be learned. A new event model (e.g. representing avalanches) is then obtained by using the widespread background model to adjust the event model description by using only one training event. In contrast to the classical HMM approach, the

classification system of this approach consists of a background model and one event model for each implemented event class. The classification process itself calculates the likelihood that an unknown data stream was generated by a specific event class for each individual HMM class (Hammer et al., 2012, 2013).

This new approach was successfully used on continuous seismic data collected at the Wannengrat field site during the 2009-2010 winter season by Heck et al. (2018a). Their classification, however, consisted of creating a new background model for each day and the resulting classification system was used to classify the data of the same day. A near real-time classification, as would be required for operational purposes, is then not possible. To overcome this problem, here we implemented a classification process by learning the background model using data from a different time window than the data we wanted to classify. To train the background model we used the ~~seismic time series as~~ pre-processed data taken from the window t_{model}, whereas the pre-processed data we want to classify are in the time window t_{class} (Figure 5). This so-called operational classification was performed by using a window length of $t_{\mathrm{model}} = 24\,\mathrm{h}$ and $t_{\mathrm{class}} = 1\,\mathrm{h}$ with the start time of t_{class} corresponding the end of t_{model}. This means, that our background model is always determined by the pre-processed data of a 24-hour window. By choosing a length of $1\,\mathrm{h}$ for the window t_{class}, we were able to classify the pre-processed continuous seismic data of one hour during one step of the operational classification. Once one classification step, which is the classification of the window t_{class} is finished, both windows are shifted by one hour and the classification was executed for the shifted windows. The so performed classification takes $\sim 6\,\mathrm{min}$ for the classification of one day without the feature calculation. In contrast, the classification performed by Heck et al. (2018a) only took $\sim 30\,\mathrm{s}$ for one day. All calculations were performed on a computer with a regularly available 8-core processor and $12\,\mathrm{GB}$ ram running a standard Ubuntu Linux Distribution.

As input for the HMMs a compressed form of the data was used, so-called features. Features represent different aspects of the time series such as spectral, temporal or polarization characteristics. ~~These are calculated using a sliding window and therefore the time series is represented in a compressed form.~~ Since we used ~~data from~~ single component geophones, we only used the following spectral and temporal features ~~suggested by Heck et al. (2018a):~~
similar to those used by Heck et al. (2018a).

- Central frequency (Barnes, 1993)
- Dominant frequency (Kramer, 1996)
- Instantaneous bandwidth (Barnes, 1993)
- Instantaneous frequency (Taner et al., 1979)
- Cepstral coefficients (Kanasewich, 1981)
- Half-octave bands (Joswig, 1994)

~~To calculate the features from the pre-processed data~~For the feature calculation, we used a sliding window of width $w = 512$ samples and a step size of $0.05\,\mathrm{s}$ or 25 samples ~~,~~resulting in an overlap of $97\,\%$. ~~In total, we used~~ We used in total 6 half-octave bands for the classification and the first half-octave band had a central frequency of $3.9\,\mathrm{Hz}$.

3.3 ~~HMM construction~~

~~The hidden Markov models we used to automatically identify avalanches in the continuous seismic consisted of a background model and an event model for each event class (Hammer et al., 2017; Heck et al., 2018a). In our application we used only one event class, either avalanches at the Dischma field site or airplanes at the Wannengrat field site.~~

~~The background model was learned by using features extracted from the~~ Calculating the features from the pre-processed ~~data. Previous work has shown that a background model which is regularly updated provides better classification results throughout a season (e.g. Heck et al., 2018a). In our case, we therefore used the pre-processed data from a 24 h window to train~~ data takes $\sim 15\,\mathrm{min}$ for a complete day for all sensors. Since we shift the windows for $1\,\mathrm{h}$ after each step of the operational classification, the ~~background model and recalculated it every hour, i.e. we used a sliding window of length $t_{\mathrm{model}} = 24\,\mathrm{h}$ and then shifted it forward by one hour (background data in Figure 5).~~

~~In contrast to the background model, the event model was only calculated once for the entire season (training event in Figure 5). For the Dischma field site, our training event consisted of a signal generated by an avalanche that had released on 9 March 2017 at 06:47 (Figure 7a), an unambiguous event that was analyzed in detail by Heck et al. (2018b). For the Wannengrat field site, our training event consisted of a signal generated by an airplane on 31 January 2017 at 21:46 (Figure 7b).~~ calculation of the features for a complete day needs to be performed only for the very first step. For the following steps it is sufficient to calculate only the features for the window t_{class} with a length of $1\,\mathrm{h}$, which approximately takes less than $\sim 2\,\mathrm{min}$ for the calculation.

3.3 ~~Classification~~

~~To classify unknown data, we used a window of length $t_{\mathrm{class}} = 1\,\mathrm{h}$ immediately following the 24 h long training window (Unclassified data in Figure 5). These data were~~ The classification process consists of five steps: pre-processing, feature calculation, HMM construction, classification and post-processing (Figure 5). First the data used to build the background model are selected from the time window t_{model} and the data to be classified are determined by the window t_{class}. The data from the selected time windows are pre-processed ~~and features were calculated. Based on these features, the HMM classification processthen calculated the likelihood that an unknown data stream was generated by a specific event class (Hammer et al., 2012, 2013). The classification was performed for each individual sensor.~~

3.3 ~~Post-processing~~

~~Since the classification algorithm is not perfect, several~~ to reduce the amount of noise and then the features are calculated. In the HMM construction part, the features calculated from the data within t_{model} and from the data of the training event are used to construct a background model $\mathrm{HMM}_{\mathrm{Back}}$ and an event model $\mathrm{HMM}_{\mathrm{Event}}$. The event model $\mathrm{HMM}_{\mathrm{Event}}$ was learned using only one training event that is representative of avalanches at a specific field site (Heck et al., 2018a). It was determined once and then applied for the entire winter season. In contrast, the background model $\mathrm{HMM}_{\mathrm{Back}}$ was reconstructed every hour. Using both models, the pre-processed data within the window t_{class} were classified in the classification process. The features

~~Avalanche released on 9 March 2017 at 06:47 used as training event for the classifier at the Dischma field site. a) time series for the 7 sensors. The red area indicates the part of the time series used as training event. b) corresponding spectrogram of the seismic time series.~~

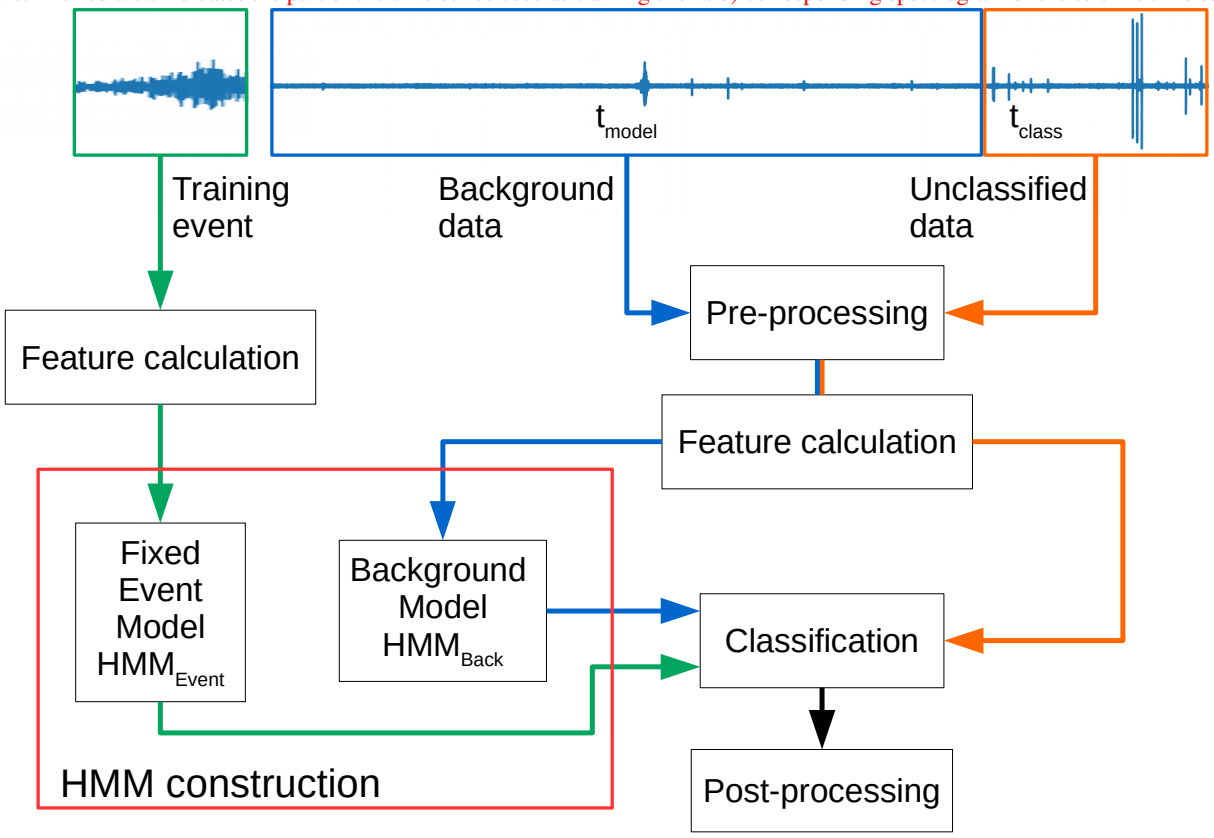

Figure 5. Flow chart of the classification process. Green lines show the construction of the event model. Blue lines show the construction of the background model. The orange lines show, how the data to be classified are processed.

calculated for this window are therefore passed to the classifiers. Once the classification is performed, post-processing steps ~~were applied to reduce the number of false detections. Detections with a duration ≤ 12 s were dismissed(Heck et al., 2018a), and we only considered an event as an avalanche when it was detected by at least five sensors of the array, as proposed by Heck et al. (2018a). Two additional steps were also implemented in the classification workflow and are described in the following~~are applied as proposed by Heck et al. (2018a). The first step consisted of applying a duration threshold to the classified events. Each classified event shorter than 12 s in duration was dismissed. The second step, the so-called voting-based classification, combines the results of all sensors. Only events that were classified by at least 5 sensors are considered as possible avalanches.

3.2.1 ~~Combined array detection~~

3.3 Combined array detection

~~Avalanche signals are typically only detected within a radius of 3 km of our seismic arrays (van Herwijnen and Schweizer, 2011b; Heck et a~~
~~Since the distance between the Dischma and the Wannengrat array was 14 km, it is therefore very unlikely that an avalanche was recorded at both arrays simultaneously. Signals that were recorded simultaneously~~ Initial classification results performed on the data set of the winter season 2016-2017 revealed that although the total number of detected events was low, many detected events were very likely generated by airplanes or regional earthquakes (local magnitude between 1.5 and 4 for earthquakes at local and regional distance triggered by at least 6 stations according to the earthquake catalog of the Swiss Seismological Service). In contrast to avalanches, which are recorded only at one array, these events are recorded at both arrays~~were thus most likely false detections. To remove such signals from the events automatically classified at the Dischma array , we implemented~~ . We therefore used a combined array detection to remove earthquakes and airplanes from the detections. To perform the combined array detection, a second HMM ~~trained with the airplane event from 31 January at 21:46 (Figure 7b) to classify~~ was implemented to identify earthquakes and airplanes in the data recorded at the Wannengrat ~~and subsequently using the same post-processing steps mentioned earlier. However, since only two sensors recorded data at the Wannengrat array, we only considered events detected by these two sensors~~array at 14 km distance from the Dischma array. Classification results ~~from the Dischma and Wannengrat arrays~~ were then combined to remove all events recorded simultaneously at both arrays~~, which means that the time difference between the detections at both field sites was less than 1 min~~.

3.3.1 ~~Source localization~~

3.4 Localization results to confirm avalanches

~~Array processing methods provide information on the signal source and can provide additional parameters to classify events as avalanches, as is commonly done when exploiting infrasound signals (Scott et al., 2007; Marchetti et al., 2015; Thüring et al., 2015). To locate the source of events, we used the MUSIC algorithm, as suggested by Heck et al. (2018b)~~Heck et al. (2018b) determined the direction of several avalanches using a multiple signal classification algorithm called MUSIC and were able to locate the avalanche path of several avalanche events based on the data of a single array. The MUSIC ~~method was applied to non-overlapping data windows for four frequency bands between 6 and 7.5 Hz to determine~~ algorithm determines the back-azimuth angle and the apparent velocity of the incoming wave-field ~~with time . The length of the windows was set to five cycles of the lower corner of the analysed frequency band, meaning that the data were divided into more windows for higher frequencies. By combining the~~ for a small time window. This time window is shifted to provide a time series of back-azimuth ~~values for all four frequency bands , we then applied~~ and apparent velocity values. The MUSIC method is based on the covariance matrix taking the data of all sensors into account at once, whereas beam-forming methods rely on pair-wise cross-correlation (Schmidt, 1986; Rost and Thomas, 2002). MUSIC can resolve multiple sources more easily than beam-forming methods. Furthermore, the MUSIC method can be applied to small frequency bands and the different frequency

contents of the wave-field can be analyzed. For further information on multiple signal classification the reader is referred to Schmidt (1986) and Hobiger et al. (2016).

Heck et al. (2018b) found, that due to the small distance between the sensors, the seismic array mostly resolved sonic wave-fields rather than seismic wave-fields to estimate the back-azimuth. Using a median smoothing filter ~~on a moving window of 8 s to determine a~~ they then calculated a so-called median back-azimuth path with time~~, as in Heck et al. (2018b) (Figure 13a).~~

~~(a)~~

~~(b)Localization results for an avalanche event recorded on 9 March 2017 at 6:47. a) polar plot representation of the back-azimuth calculated using the MUSIC method. Red dots are the back-azimuth values for a single time window. The black line represents the median back-azimuth path. The solid part of the line has variations below the threshold value for the derivative, whereas the dotted line refers to strong variations. b) derivative of median back-azimuth path. The dotted lines represents the threshold value of 10°. The part between 52 s and 113 s corresponds to the solid line in a).~~

~~To~~ . In this study, we used these median back-azimuth paths obtained by the event localization to decide whether a classification was associated with an avalanche~~or not, we applied~~ . Specifically, we used a threshold value ~~to~~ for the derivative of the median back-azimuth path. The assumption ~~was~~ is that avalanche events have a ~~relatively~~ smooth median back-azimuth path with little variations, whereas false detections ~~show larger variations in back-azimuth, which is also the case for earthquakes and airplanes for our specific array geometry. Indeed, the training event at the Dischma array had a duration of around 50 s and a median back-azimuth path with slight changes in the angle (black line in Figure 13 a) whereas before and after the event , the~~ have randomly distributed back-azimuths ~~were more erratic, as expected for noise. For the training event , the derivative of~~ with large variations in time. By analyzing several avalanche events, especially the events identified by Heck et al. (2018b), we observed small changes below 10° for the ~~median~~ back-azimuth ~~path stayed below~~ path. Hence, we used a threshold value of 10° ~~for 50 s, while before and after the event it was much larger (Figure 13b). Other avalanche events had very similar results(not shown). Events with derivatives of the~~ between two adjacent points of the median back-azimuth ~~path smaller than 10° for a minimum duration of 20 s were then classified as avalanches. Since we used 8 s windows for the calculation of the~~ path for the event detection. Even for events passing close to the array, we observed changes below 10° in the median back-azimuth ~~path, we had to increase the minimal event duration to~~ path. Heck et al. (2018a) suggested that a detected event should have a minimum duration of 12 s to be considered as an avalanche. For the localization step, however, it was necessary to increase this duration because the window length used for the median smoothing filter was already 8 s long (Heck et al., 2018b). To cover enough data points to use the minimal event duration as a reliable classification criterion, we therefore required a minimum length of 20 s for the back-azimuth path. Heck et al. (2018b) also showed that only the frequency content of the signal between 4.5 and 12.5 Hz contained information valuable for the localization performed at the used array. By further analysis of the already localized events by Heck et al. (2018b), we observed, that a reduced frequency range provided similar results. Hence we reduced the number of analyzed frequency bands to four bands between 6 and 7.5 Hz and were able to speed up the calculation time. Nevertheless, the processing time for the localization is about three times real time on the same computer used for the classification as mentioned earlier.

4 ~~Results~~Classification results

We ~~applied our automatic avalanche detection workflow on~~ performed the avalanche detection for the data recorded at the Dischma ~~field site from 1 January to 30 April 2017. We then~~ array during the winter season 2016-2017 and compared the results with ~~an avalanche catalogue obtained by visual observations from local observers~~ the avalanche activity visually obtained by local observers and compiled by the avalanche warning service at the SLF. ~~The visual observations in the area of Davos can be incomplete and cover~~ It has to be noted that this compilation is incomplete and covers an area much larger than ~~the area monitored with our seismic system at the Dischma site~~that monitored with the Dischma array. Therefore, comparison with this ~~avalanche catalogue~~ compilation remains indicative.

4.1 Overview of the winter season

The winter period of 2016-2017 was relatively short and characterized by a below-average snow depth. First snowfalls were quite late in the season, in the middle of December, followed by four weeks without substantial precipitation and low temperatures. ~~As the thin snowpack was subjected to large temperature gradients for an extended period of time~~Due to the constant high temperature gradient within the snowpack, a poorly bonded layer of depth hoar was formed at the base of the snow cover.

During the winter season, ~~four pronounced~~ three significant snowfall periods occurred~~: between 1 and 15 January, around 1 February, from 1 to 10 March and around 15 April~~ ; one in each month from January to March (increase of blue line in Figure 6). Each ~~snowfall was associated with increased~~ of these snowfalls were associated with considerable avalanche activity in the region of Davos ~~, except the snowfall in April~~ (red bars in Figure 6~~b~~).

In addition to these ~~visual avalanche observationsby local observers, we inspected~~ avalanche observations, we analyzed the pictures taken by the automatic cameras installed at ~~the Dischma field site~~our field sites. Surprisingly, avalanche activity was ~~very low~~ low at the Dischma field site in January and February~~, and only a few avalanches were identified on 1 February 2017.~~ . During the early March snow storm ~~,~~ the visibility was poor and only very few avalanches were identified on the images of the automatic ~~cameras~~camera. However, once the storm ~~had passed~~was over, the intensity of the avalanche cycle became clear as many avalanche deposits were visible on the images. Five days after the storm we mapped 24 avalanches within a $4\,\mathrm{km}$ radius of the Dischma field site ~~(for more details see Heck et al., 2018b). Later in the season, we did not observe any more avalanches on the images. Thus, the avalanche cycle between 9 and 10 March was the most prominent avalanche period at the Dischma field site.~~ (Heck et al., 2018b).

4.2 Classification performed at single array

~~Using the classifier trained with the avalanche event from~~ The main classification was performed at the Dischma field site for all seven sensors. Based on the visual inspection of the seismic data performed by Heck et al. (2018b), several avalanche events suitable as training events for the HMM were identified. However, they had mainly analyzed the period of high avalanche activity on 9 and 10 March 2017. Visually inspecting the entire winter season we identified 44 avalanche events. However, as already shown by Heck et al. (2018a), visually inspecting seismic data contains many uncertainties. An avalanche released

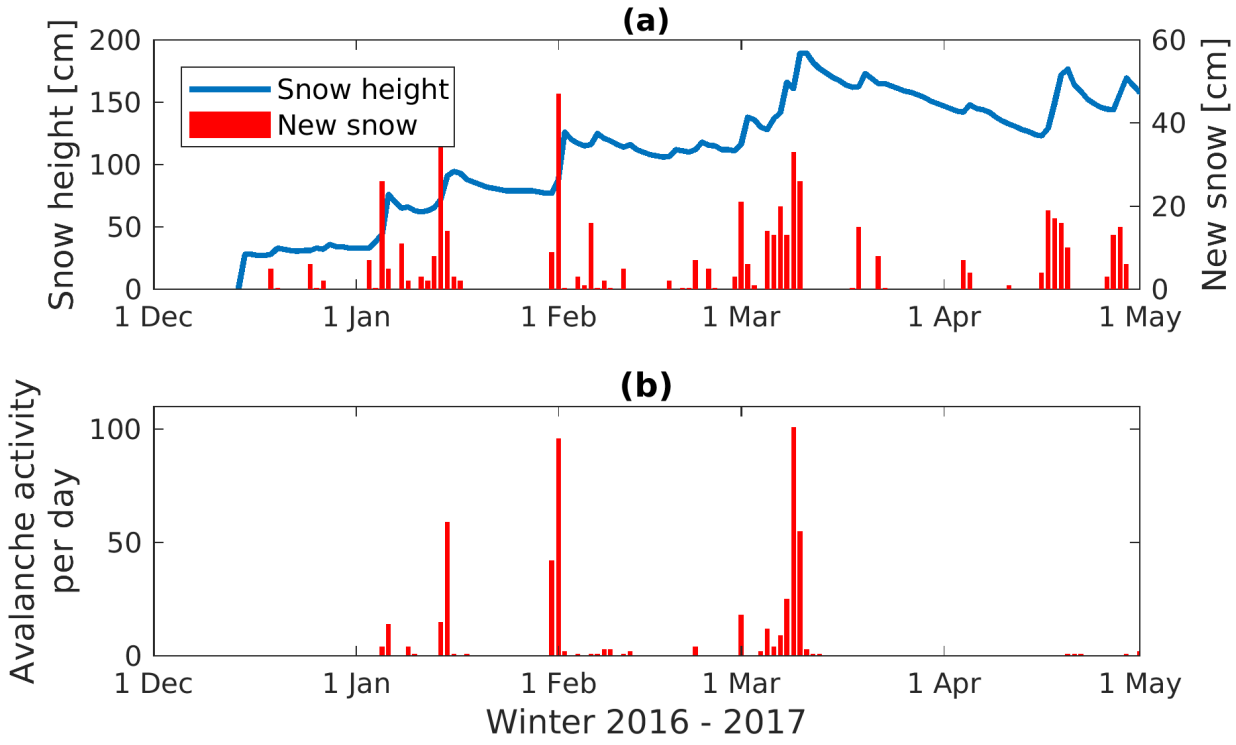

Figure 6. a) Snow height measured at the automatic weather station at Weissfluhjoch 12 km to the northwest of the Dischma array at ~~2540 m~~ ~ 2600 m a.s.l. for the winter season 2016-2017. ~~Orange~~ Red bars are the height of new snow measured each day at 8:00 am. b) Number of avalanches observed per day in the region of Davos ($\sim 175\,\mathrm{km}^2$).

on 9 March 2017 at 06:47 was already analyzed in detail by Heck et al. (2018b) and can unambiguously be classified as an avalanche. We therefore decided to use this event as our training event (Figure 7~~a), we classified the data from~~).

Using the classifier trained with this event, we performed the classification for each single sensor of the ~~Dischma array and post-processed the results to remove events~~ array. In a next step, the results of the classification were post-processed; first all results of each sensor with a duration $\leq 12\,\mathrm{s}$ ~~and~~ were dismissed (Heck et al., 2018a). Finally we dismissed all classifications that were classified by less than 5 sensors. ~~This resulted in~~

The classification and the following post-processing was applied to the continuous data set recorded from 1 January to 30 April 2017. For this period, a total of 117 ~~automatically detected events between 1 January and 30 April 2017 (Figure 8)~~events were classified as avalanches. A quarter of the events were detected by 5 sensors, a quarter by 6 and about half by ~~7 sensors.~~

~~Classification results after post-processing (including voting-based classification) at the Dischma array. The colored bars indicate the number of classified events per day depending on the number of sensors: Violet bar indicates detections by 7 sensor, turquoise bars by 6 sensors and yellow bars by 5 sensors.~~

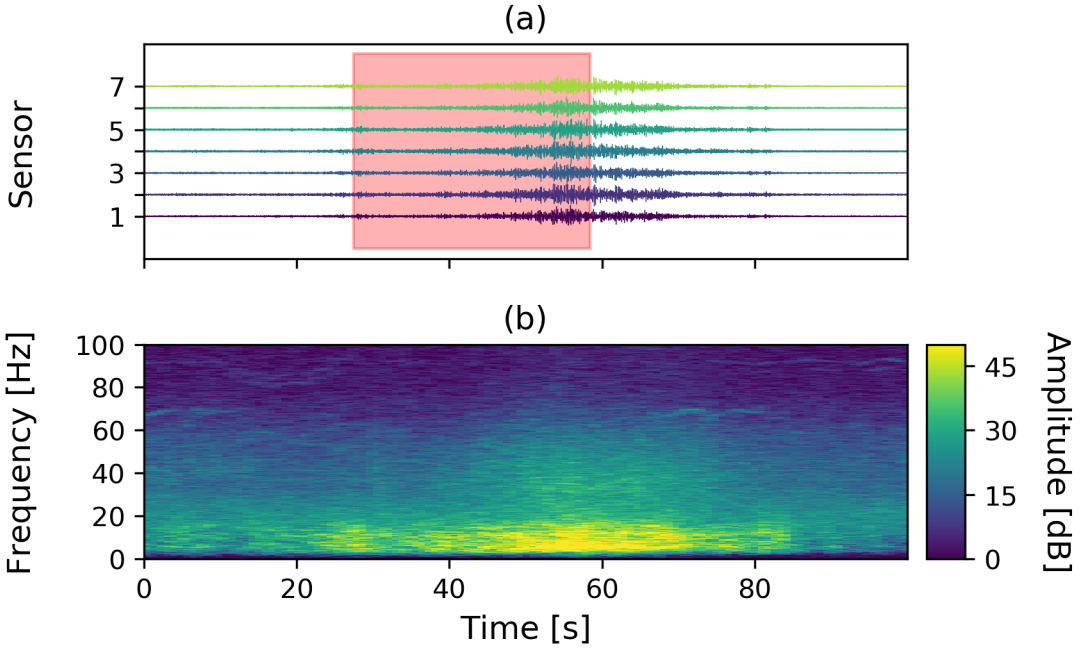

Figure 7. Avalanche released on 9 March 2017 at 06:47 used as training event for the classifier. a) time series for the 7 sensors. The red area indicates the part of the time series used as training event. b) corresponding spectrogram of the seismic time series.

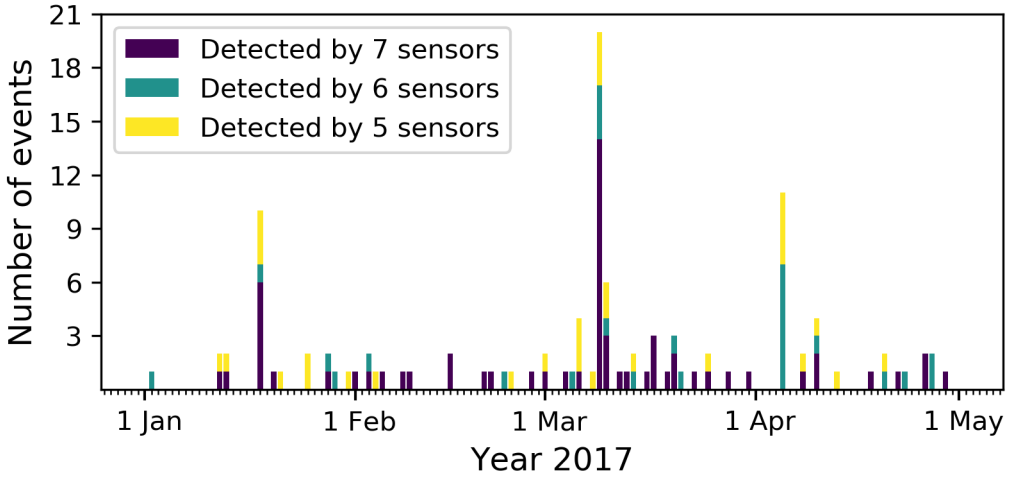

Figure 8. Classification results after post-processing (including voting-based classification) at the Dischma array. The colored bars indicate the number of classified events per day depending on the number of sensors: Violet bar indicates detections by 7 sensor, turquoise bars by 6 sensors and yellow bars by 5 sensors.

Most events occurred 7. Most events were classified during the early March snow storm on 9 and 10 March 2017. In addition , peaks 2017 (Figure 8). In addition a peak in the middle of January and early April were beginning of April and a cluster of events around the beginning of February was visible. The peak in January corresponded as well as the cluster around the beginning of February correspond with the avalanche activity period visually recorded in the region of Davos (Figure 6). For the peak in April, however, no avalanches were observed in the area surroundings of Davos. Furthermore, several single detections were distributed over the season showing no clear link to the avalanche observations in the region of Davos. We therefore accordance with the visual avalanche observations. Therefore we visually inspected the time series and the corresponding spectrograms of each of the 117 classifications and found that the HMM also classified ~ 50 various airplanes (Figure 9 a)) and regional earthquakes (Figure 9 b) as avalanches.

Although these misclassified events can be distinguished from avalanches through visual inspection (e.g. the sharp onset visible for earthquakes), the classifier identified these events as belonging to the avalanche class. We attribute these false classifications to the fact that these , even when we used different training events or varied the setup for the classification (results not shown). This was most likely because earthquake and airplane signals were more similar to the avalanche training event avalanches than to the background model. Indeed, the temporal trends in the features exhibited many similarities (Figure 10). Using different training events did not substantially change these results (not shown). , and consequently tagged as avalanches.

Analyzing the features also showed the similarities of the different types of events, especially the time dependent behavior. In the beginning of the event, the feature behavior of the events is different, however, at the end of the event a similar time dependent behavior is visible (Figure 10). Due to theses similarities, airplane and earthquake events are more similar to avalanches than to noise resulting in false classifications of these events.

4.3 Classification performed at both arrays

The vast majority of the misclassifications were produced by two types of events: , i.e. airplanes and earthquakes. A comparison of several detected earthquake events with the earthquake catalog of the Swiss Seismological Service (SED) showed, that all compared earthquake events occurred within a range of 120 km. As the Wannengrat array was deployed only 14 km away, all observed earthquakes were likely to be detected simultaneously at both arrays. Moreover, Davos lies within an approaching corridor of the international airport Zürich and numerous several commercial airplanes pass by every hour at an altitude of at least 5 km. Similar to avalanches, airplanes also have a moving source character . However, and due to the high altitude (typically > 5 km) and fast movement of the source, airplanes are likely recorded fast movement they are also observed almost simultaneously at both arrays. Furthermore, based on the earthquake catalog of the Swiss Seismological Service (SED), we concluded that regional earthquakes within a range of 120 km were recorded by both arrays. Airplanes and earthquakes were therefore recorded almost simultaneously at both arrays (Figure 9). To eliminate these false classifications, we thus used data from Indeed, a comparison of both time series revealed that earthquakes were recorded at both arrays at the same time whereas airplanes were recorded with a small delay of 20 to 30 s due to the movement of the source. The time series and spectrograms at Dischma and Wannengrat were very similar (Figure 11).

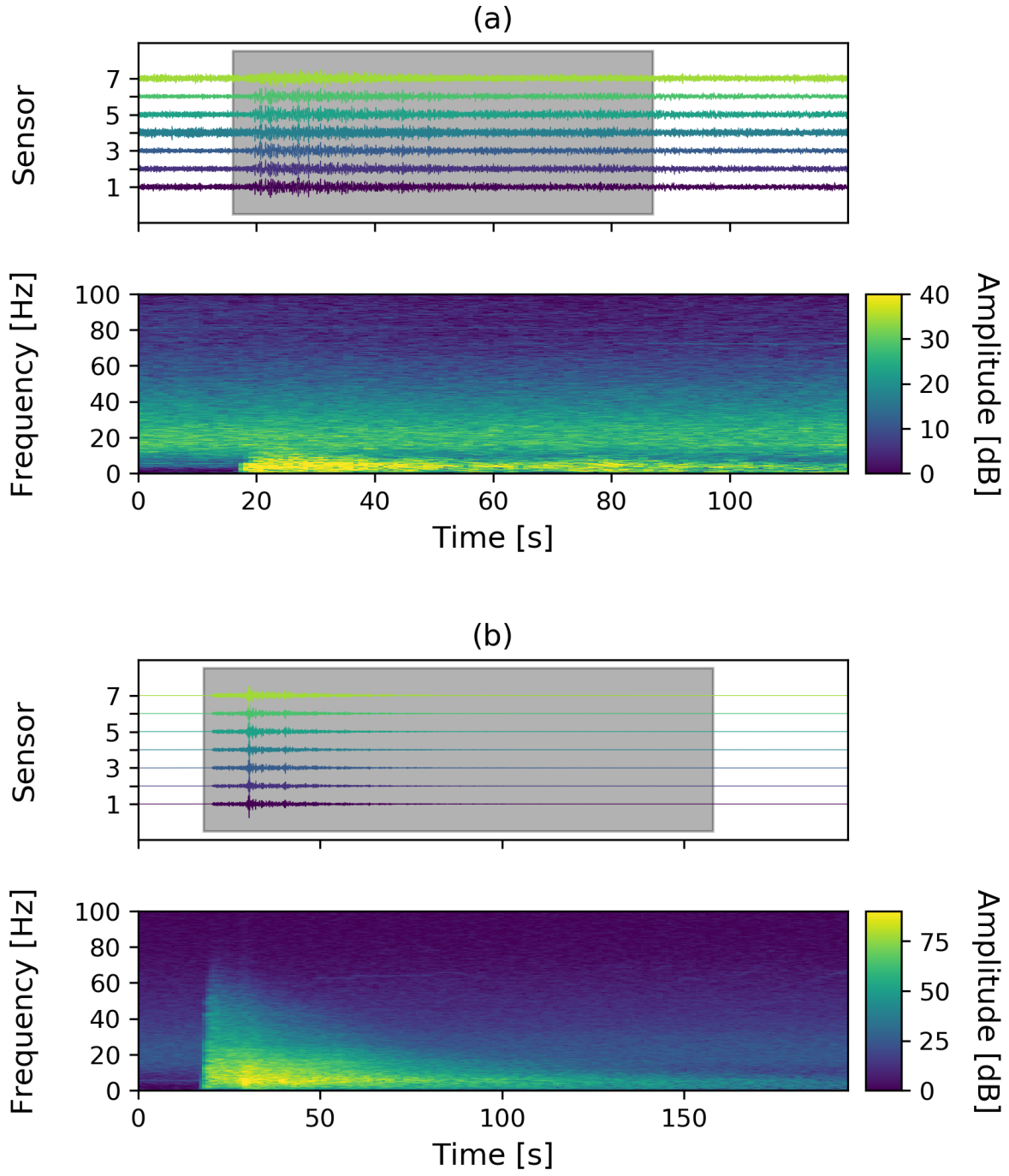

Figure 9. Time series and corresponding spectrograms for two false classifications, ~~airplane detected at~~ a) ~~Dischma and~~ airplane, b) ~~at Wannengrat and an~~ earthquake~~detected at c) Dischma and d) Wannengrat~~. The gray rectangular area indicates the part classified as event by the HMMs.

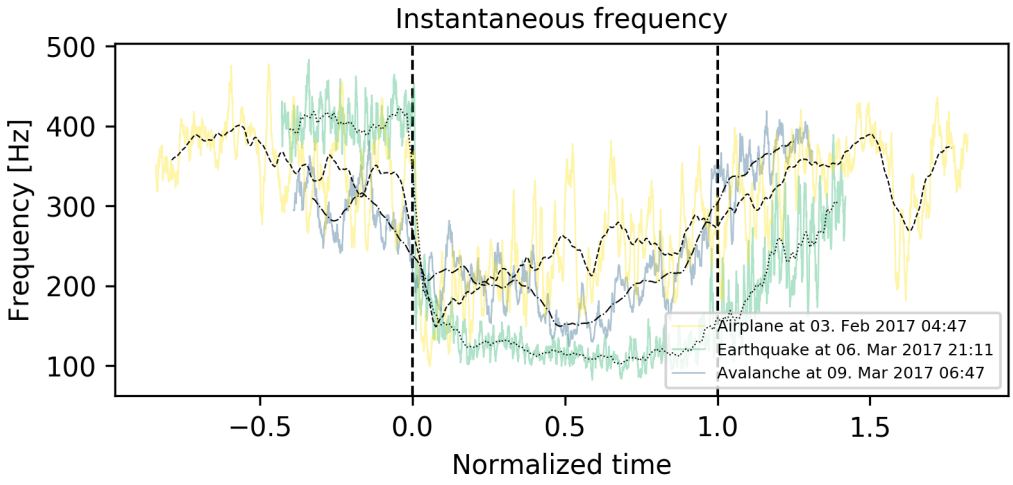

~~Instantaneous frequency with normalized time (normalized with event duration) for signals generated by an airplane (yellow), an earthquake (green) and an avalanche (blue). The black lines are the moving mean. The black vertical dashed lines at 0 and 1 indicate the start and the end of the events.~~

Figure 10. Feature instantaneous frequency for three different event types, yellow represents the signal produced by an airplane, green of an earthquake and blue of an avalanche. The black lines are the mean of the features. The dashed line at 0 indicates the start of the events and the dashed line at 1 the end of the event.

Avalanche signals, however, were only detected within a radius of 3 to 4 km of the array and were therefore only recorded at one array (Heck et al., 2018b). In order to eliminate classified events recorded at both arrays, we performed a second classification at the Wannengrat array~~classified with the~~. Due to similarities of the transient signals as mentioned earlier, a HMM trained with ~~the airplane event of 31 January at 21:46 (Figure 7b). As the transient signals of airplanes and earthquakes were very similar (Figure 10), this HMM also detected earthquakes.~~

an airplane signal was capable to also detect earthquakes. A closer look at the classification results for the Wannengrat array revealed, that it was sufficient to only use the HMM trained with an airplane signal (not shown here). The number of detected events at ~~the Wannengrat array varied~~ this array varies strongly per day (blue bars in Figure 12). ~~53 of these events coincided with events classified at~~

The start times obtained by the secondary classification performed with the Wannengrat data were then compared with the classification results for the Dischma array~~and were dismissed as false detections~~. Overall, 53 of the 117 classifications were detected almost simultaneously at both arrays and we considered theses events as airplanes or earthquakes (yellow bars in Figure 12~~and Table ??). The remaining~~). After the comparison of the classification results obtained by both arrays 64 potential ~~avalanches were again mostly concentrated in January, around 9 and 10 March and early April~~avalanche events remained (turquoise bars in Figure 12). The distribution of these events ~~was somewhat~~ is similar to visually observed avalanches (~~compare to red bars in~~ Figure 6), except for ~~the detections in April and the absence of~~ detections at the beginning of April

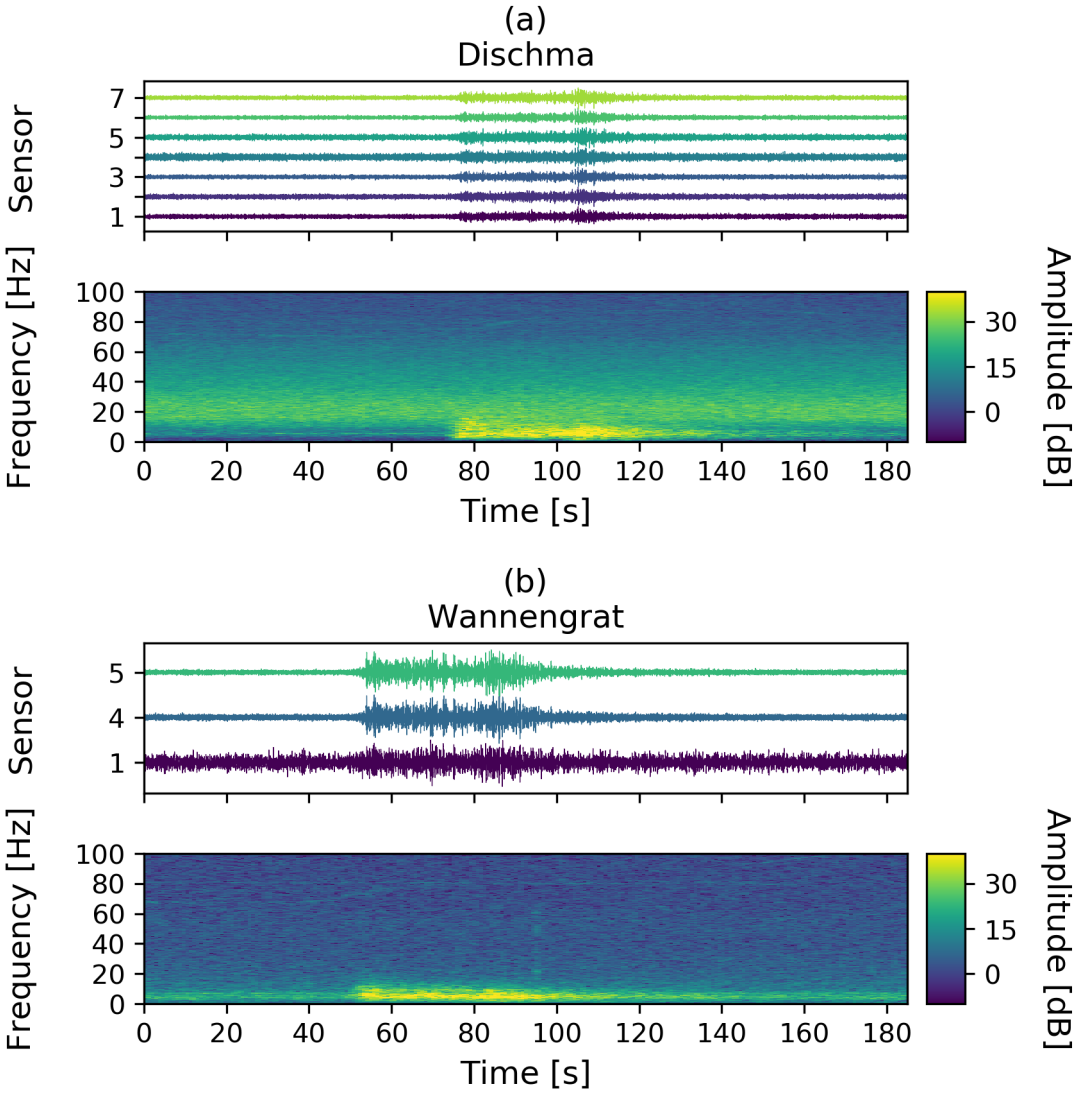

Figure 11. Time series and corresponding spectrograms of an airplane detected at both arrays on 28 January 2017 at 9:17. a) shows the signal recorded at the Dischma array and b) at the Wannengrat array.

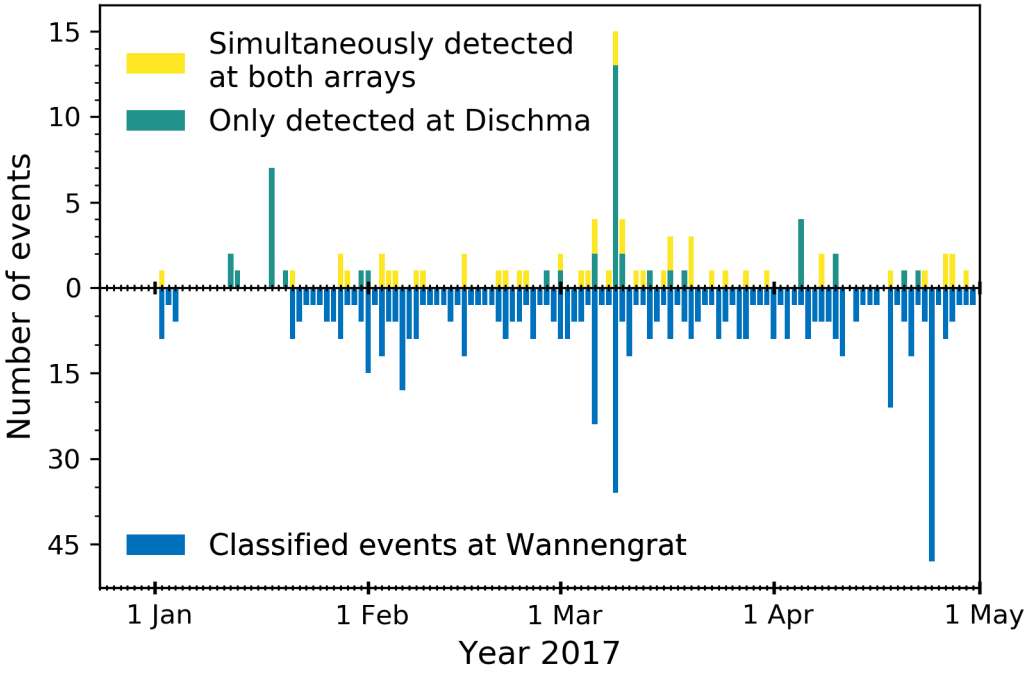

Figure 12. Yellow bars indicate the number of events detected at both arrays and turquoise bars only events recorded at the Dischma array. Blue bars are the number of airplanes and earthquakes detected at the Wannengrat array. Between 5 and 20 January no data were recorded at the Wannengrat array due to technical issues.

and no detections at the beginning of February. These events were only detected using the automatic classification approach. Furthermore, due to the previously mentioned acquisition problem of the Wannengrat array, all events between 12 and 20 January 2017 were considered as avalanches as we had no further information from the second array. Hence, we expected some misclassifications among the remaining 64 avalanche events.

~~Number of events during the season. Yellow bars indicate the events detected at both arrays, the turquoise bars show the events only recorded at the Dischma array. Blue bars show the events automatically detected at the Wannengrat array. Between 5 and 20 January no data were recorded at the Wannengrat array.~~

~~single array combined detection location based detection total analyzed 117 64classified as avalanche 117 64 21dismissed 53 43~~

~~Number of analyzed events, events classified as an avalanche and dismissed events for the different steps in the classification workflow. For the single array classification, the total number of analyzed and dismissed events cannot be provided as the entire time series was classified.~~

4.4 Localization post-processing

We In a last processing step, we applied the MUSIC method to the remaining 64 classified events to determine the estimate the back-azimuth and to find a possible median back-azimuth paths. Events with derivatives in the path. The event used to train the HMMs had a duration of around 50 s showing a median back-azimuth path with slight changes in the angle (straight black line in Figure 13 a). Before and after the event, however, the back-azimuths were randomly distributed as would be expected for noise. For the training event, the derivative of the back-azimuth path has low values for the 50 s part with a median back-azimuth path larger than with small changes (Figure 13 b). For this 50 s long interval, changes below 10° were dismissed. observed for the median back-azimuth path. Before and after the event, however, the changes are very high due to the randomly distributed back-azimuths. Further analyzed avalanche events also had changes of the back-azimuth below 10° and we therefore set the 10° as a maximum threshold value. Doing so, another 43 37 events were dismissed and only 21 events remained(Figure 14; Table **??**). The majority of these events (i.e. 13 of 21) were observed on 27 avalanche events remained. 15 of the remaining avalanche events were observed during 9 and 10 March 2017 , while the other events showed no clear link to the visual observations (red bars in Figure 14).

Turquoise bars are the number of events per day which are locatable and are considered as avalanches. Yellow bars are the number of events per day which could not be located and were therefore dismissed. Red bars are the number of avalanches visually observed in the area of Davos.

and some events were detected during the other periods of considerable avalanche activity in February (Figure 6). Furthermore, another 10 single events were also confirmed. For each of the 21 27 events we determined a mean back-azimuth, which is the mean direction the signals came were coming from. The mean back-azimuths were all pointing towards the surrounding slopes where we expected avalanches to release (Figure 15). Events with a duration longer than 100 s were detected coming either from the north-west or south-east.

Apart from analyzing only the events remaining after the combined array classification, we also performed the localization post-processing for those 53 events we had dismissed. Based on the localization, 48 events were again dismissed, but 5 had a median back-azimuth path within the threshold value. Hence, by directly applying the localization step 32 avalanche events remained, but including at least 5 false detections (15 %).

5 Discussion

Machine learning algorithms are increasingly used for automatic signal detection in seismic data, in particular when investigating gravitational mass movements such as landslides, avalanches, rockfalls and debris flows. They include neural networks (Perol et al., 2018; E deep learning (Ross et al., 2018), random forest classifiers (Li et al., 2018; Provost et al., 2016), nearest neighbors (Bessason et al., 2007) o kurtosis-based picking (Hibert et al., 2014). While with appropriate calibration these methods generally perform rather well, the main drawback is that a large pre-labelled training database is required. The same is true for signals generated by snow avalanches (e.g. Rubin et al., 2012). The classification workflow we presented

(a)

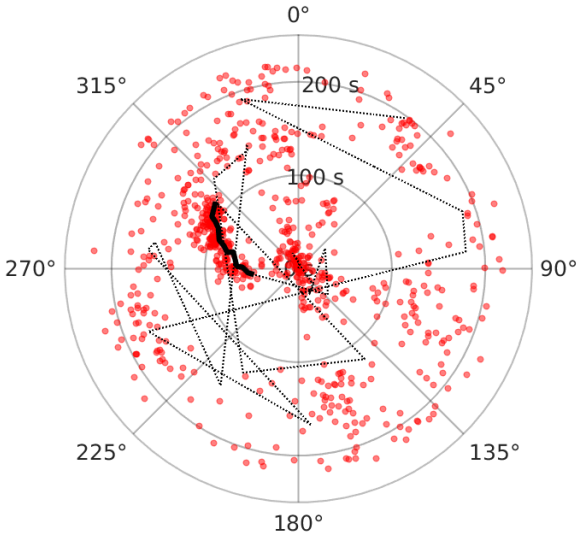

(b)

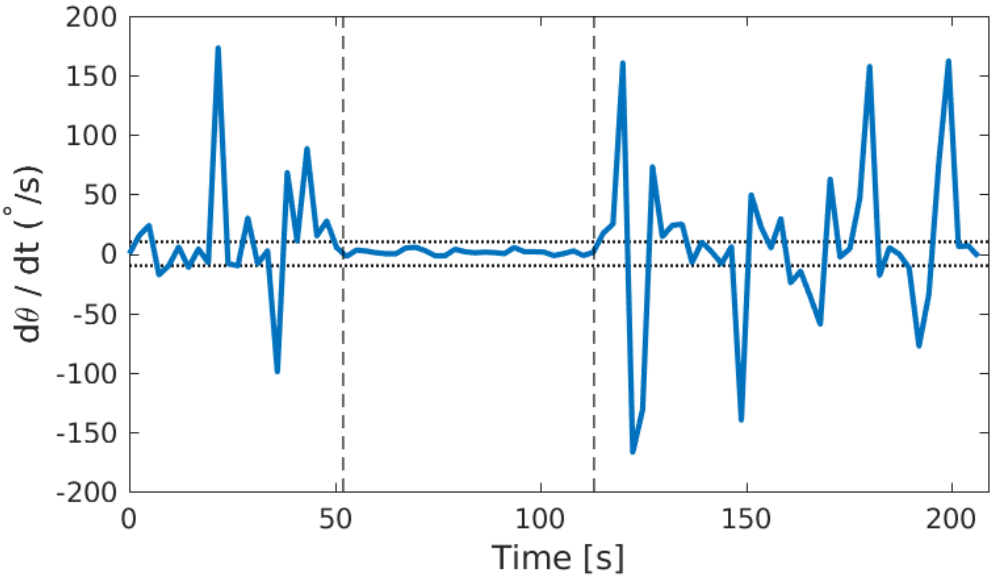

Figure 13. Localization results for an avalanche event recorded 9 March 2017 at 6:47. a) polar plot representation of the back-azimuth calculated using the MUSIC method. Red dots are the back-azimuth values for a single time window. The black line represents the median back-azimuth path. The solid part of the line has variations below the threshold value for the derivative, whereas the dotted line refers to strong variations. b) derivative of median back-azimuth path. The dotted lines represents the threshold value of 10°. The part between 52 s and 113 s corresponds to the solid line in a).

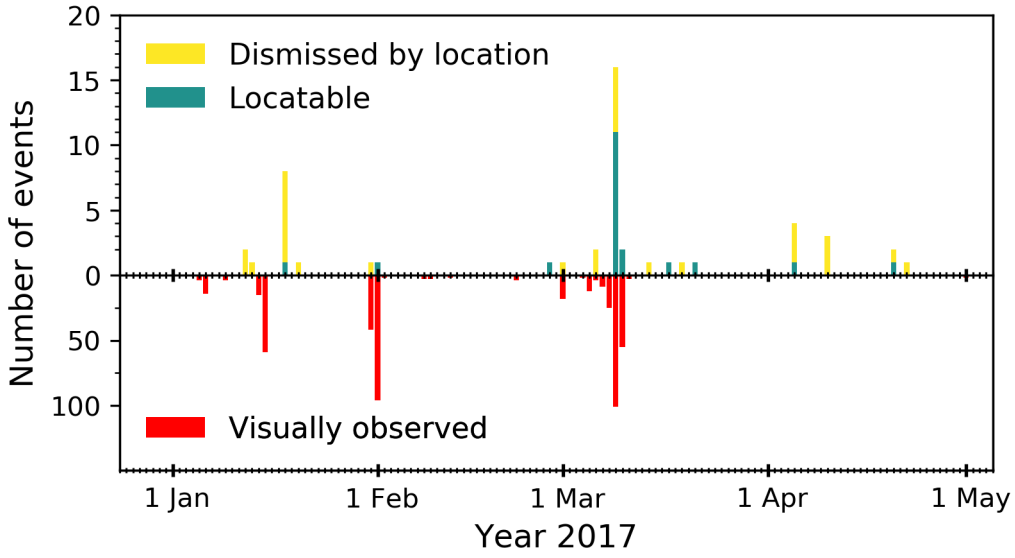

Figure 14. Turquoise bars are the number of events per day which are locatable and are considered as avalanches. Yellow bars are the number of events per day which were not locatable and therefore dismissed. Red bars are the number of avalanches visually observed in the area of Davos.

We used hidden Markov models (HMMs), a machine learning algorithm, to automatically detect avalanches in data from seismic systems deployed above Davos, Switzerland. The approach builds on the work of Heck et al. (2018a), who adapted the HMM method developed by Hammer et al. (2017) to detect avalanches in continuous seismic data from a small aperture geophone array. ~~A major benefit of this approach is that only one training event is required. This has substantial advantages, as the workflow could be implemented at a newly instrumented site without the need to first establish an extensive training data set. Still, a pre-operational training phase, typically one winter season, is needed to acquire at least one training event and to identify any site-specific peculiarities. Using training events recorded at different arrays might be unreliable due to possible differences in the instrumentation or heterogeneities in the local geology~~Using their approach on our data resulted in automatic detections that still contained a large number of falsely classified events because only one event type (avalanche) and the background noise was used for the classification with HMM. Earthquake and airplane signals have characteristics closer to avalanches than the background noise, and were therefore included in the detections.

~~For the training event, we only used the first section of the avalanche signal, up to the maximum amplitude (Figure 7). Using the entire length of the avalanche signal resulted in poorer classification results (not shown) as there were very little variations in the transient feature behavior after the maximum in the signal. Including larger parts of the training event therefore did not provide any useful additional information for the classification~~ By combining the classification results with a classification performed at a second array located 14 km away, simultaneously recorded events such as local earthquakes and airplanes could

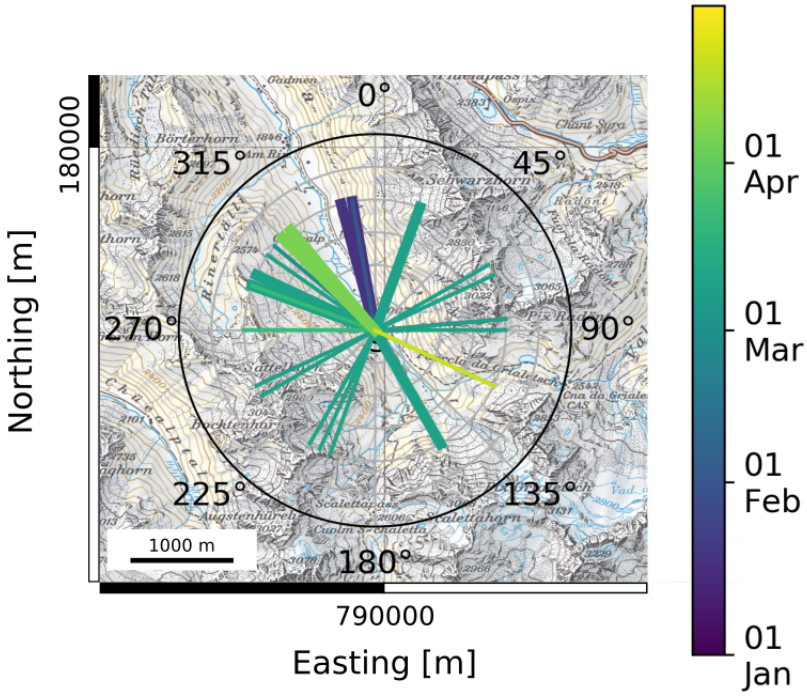

Figure 15. Polar plot representation overlaid on a map section of the field site. The angle represents the direction of the origin of the event, thin lines represent events with a duration $< 60\,\mathrm{s}$, thick lines events with duration $\geq 60\,\mathrm{s}$. The different colors of the lines represent the time of the year. Reproduced by permission of swisstopo (JA100118).

be dismissed. In addition, we applied the multiple signal classification (MUSIC) method to estimate the back-azimuth of the detected events to eliminate false alarms. Overall, this work flow allowed us to automatically identify 27 events that were very likely generated by avalanches, as the temporal trend corresponded well with the avalanche activity for the region of Davos obtained through conventional visual field observations (Figure 6 and 14). It was not possible to confirm any event with visual observations since most avalanches released during periods of bad visibility. However, Heck et al. (2018b) manually identified 13 avalanches during 9 and 10 March 2017, 12 of which were automatically identified with the approach presented here.

Apart from HMMs, several other machine learning techniques are suited to classify signals in seismic data. It is possible to use a convolutional neural network for earthquake detection and location (Perol et al., 2018) or to pick the P-wave arrival of seismic wave fields (Ross et al., 2018). Comparable to the classical HMM approach, these studies rely on large pre-labelled training data sets. Another approach is the so-called Random Forest classifier, which can be used to discriminate seismic waves (Li et al., 2018). Automatic classification approaches are also suitable to differentiate between earthquakes and quarry blasts (Hammer et al., 2013) or to characterize larger rockfalls (Dammeier et al., 2016). Further mass movements, such as landslides,

can also be identified in the seismic data based on automatic classification approaches (Esposito et al., 2006; Hibert et al., 2014; Provost et a

The automatic classification of avalanches yet remains a difficult task. Rubin et al. (2012) used several machine learning algorithms to identify avalanches in seismic data and compared the results obtained with the different approaches. With all methods a high probability of detection was achieved, but the number of false alarms was too high. A recent study by Heck et al. (2018a) showed that HMMs are a suitable tool to detect avalanches, but there is still a need for additional post-processing steps. The work presented here confirms that HMMs in combination with further post-processing steps provide reliable classification results.

~~Heck et al. (2018a) highlighted difficulties~~ In addition, Heck et al. (2018a) highlighted the difficulty in obtaining a reliable classifier ~~with the HMM approach applied to~~ trained on data from a geophone array ~~. They obtained~~ very similar to the one used in this work. Their results showed that there were large differences in model performance between the sensors, with the number of detections per sensor ranging from about 150 to over 2000. This was attributed to local heterogeneities as the sensors were packed in a ~~styrofoam~~ Styrofoam housing and inserted within the ~~snow~~snowpack. Heck et al. (2018a) therefore suggested to deploy the sensors below the snow cover and either on or below the ground. In our deployment, the geophones were buried about half a meter below the ground on a flat meadow. This approach was successful as it resulted in a much more consistent number of detections per sensor, ranging from 125 to ~~169, showing that~~ 169. Clearly, the deployment strategy can have a substantial influence on the performance of the classifier.

~~Applying the post-processing steps suggested by Heck et al. (2018a) to remove events with a duration $\leq$ 12 s and all classifications that were classified by less than~~ In contrast to the classification approach used by Hammer et al. (2017), who used a fixed background model as they analyzed a relatively short period (5 ~~sensors resulted in~~ days), we used an approach more suited for operational purposes. Indeed, for the operational set-up the background model was determined using 24 hours of data prior to the hourly data that were classified. In combination with the post-processing steps related to signal duration and number of sensors the events were detected as suggested by Heck et al. (2018a), the HMMs identified 117 possible avalanche events (Figure 8). Even though this approach identified the main avalanche cycle in March 2017 (compare Figure 6 and Figure 8), visual inspection of the classified events indicated that at least 50 % of the events were false alarms produced by distant airplanes or regional earthquakes (Figure 9). ~~Although we did not perform an exhaustive sensitivity study, some ad-hoc testing showed that these classification results did not substantially change when~~ Even by training a classifier with different feature combinations, changing the training event and/or the length of the training event, the classification results did not substantially change and airplanes and earthquakes were still classified as avalanches. This highlights the difficulty in training an accurate HMM for low energy signals generated by avalanches. ~~Based on our results, we~~ We concluded that using HMMs to automatically identify avalanches in seismic data from our geophone array will inherently contain false detections, as the ~~transient~~ overall feature behavior from distant airplanes or regional earthquakes was very similar to signals generated by avalanches (Figure 10).

To circumvent the problem of developing an optimal event classifier for one specific array, we made use of a second array at the Wannengrat. There we performed a second classification to automatically identify airplanes and earthquakes using an event model trained ~~with~~ by an airplane event. Since transient signals produced by earthquakes, airplanes or avalanches have

similarities~~(Figure 10)~~, the results obtained for the second classification based on the airplane event model ~~likely also include~~ also falsely identified avalanches and earthquakes. ~~However, this was not a drawback since we assume that it was very unlikely that two avalanches released simultaneously at both field sites. Typically, signals generated by airplanes either have clear overtones or at least a clear Doppler effect in the signal (van Herwijnen and Schweizer, 2011a). The airplane signals that were falsely classified as avalanches with our method did not have such obvious features (Figure 9). While we do not know why and when airplanes generate such signals, and we have not identified a clear pattern explaining their presence, we have seen multiple signals like these~~ Hence, a classification performed with only one event model was sufficient. The assumption for the second classification was that most falsely classified events were recorded at both arrays~~and we are confident that these signals are generated by airplanes~~. Comparing the time series of detected events at both arrays allowed us to dismiss about 50 % of the classified events (Figure 12). ~~In our case, identifying~~ Identifying co-detections across arrays is therefore an efficient approach to reduce the number of false alarms~~, as the weak signals generated by~~ . Although it was possible, that the classification results of the second array contained avalanche events, it was unlikely that two avalanches released simultaneously at both field sites. Furthermore, avalanches were only recorded at one array since the distance between both arrays was about 14 km. In the future, a promising approach could be to reduce the distance to about 2 or 3 km, as this could also help improve the localization.

~~Combining the classification results from two separate arrays~~ Although the combination of two arrays for the classification allowed us to reduce the number of false ~~classifications. Nevertheless~~classification, some uncertainty remained about the origin of the identified events. In a final step, we therefore used the MUSIC method to estimate the median back-azimuth path, as suggested by Heck et al. (2018b), to further dismiss false detections. Similar approaches were suggested for the automatic detection of avalanches in infrasonic data by Marchetti et al. (2015) and Thüring et al. (2015). In those studies, the back-azimuth of continuous infrasound data was calculated on the fly using cross-correlation techniques, and only events with slight changes in back-azimuth over a predefined minimal duration were assumed as avalanche events. In contrast, ~~we~~ here we only determined the back-azimuth ~~with the MUSIC method only for those events that were already~~ for events automatically identified by the HMM ~~, since~~ with the MUSIC method, as Heck et al. (2018b) showed that for our instrumentation pair-wise cross-correlation technique (beam forming) did not result in robust back-azimuth estimates~~for our instrumentation (Heck et al., 2018b)~~. This last processing step further reduced the number of classified events to ~~21~~ 27 (Figure 14). We also found out, that the MUSIC method would have been sufficient to determine the reliability of a detection as it was not possible to locate airplane or earthquake events with our array. After applying the localization based step to all detections, 32 events were identified as avalanches, 5 more events compared to the combined array and the localization based classification.

~~The majority of the remaining 21 automatic~~ After applying the combined array classification and the MUSIC method to the data, 27 classification remained for the winter season 2017. Nearly all of these classifications occurred during ~~a period which coincided with the~~ periods of observed high avalanche activity ~~in March~~ (Figure 14). However, ~~very few avalanches were automatically detected during~~ for the first two ~~avalanche periods observed in the surroundings of Davos~~ periods of high avalanche activity in January and February only few events were detected, whereas in the surroundings of Davos many events were observed. This may be due to fact that the Dischma site is located about 12 km ~~km~~ to the southeast of Davos ~~where avalanches are regularly observed~~ and weather and snow conditions are sometimes different since major storms arrive from

the northwest. Indeed, based on the images from the automatic cameras, very little avalanche activity was observed in the area in January and February~~, suggesting that there was only one main avalanche period at our site in March. With our automatic classification~~. Nevertheless, it was ~~thus~~ possible to reconstruct the ~~main~~ avalanche activity period in March based on the automatic classification. Results from the localization showed that during the season avalanches released from many different slopes at the field site ~~, in particular for the avalanche period in March~~ (Figure 15). This could be observed especially during the snow storm in March. A seismic monitoring system is therefore a suitable tool to monitor ~~an area with many slopes~~ a wide area and not just one single slope. Although the detection range is with 2 - 3 km rather ~~limited (Heck et al., 2018b) , the seismic monitoring~~ small (Heck et al., 2018b) the seismic system in combination with an automatic classifier provides great potential to identify ~~at least~~ the major avalanche periods. ~~These results suggest that the detection capabilities of seismic monitoring systems are very similar to those of infrasound monitoring systems (?).~~

Although we were able to identify one major avalanche activity period in the winter season ~~2016-2017~~2016 - 2017, the method presented here has its limitations. ~~Our suggested workflow requires two arrays to eliminate falsely classified events by finding co-detections. This is clearly a limiting factor as it increases the cost for the instrumentation as well as deployment and maintenance time. However, we could have directly applied the MUSIC method to all detections from the Dischma array to reduce the number of falsely classified events. Indeed, after applying the localization based step to all detections, 32 events were identified as avalanches , 11 more than with the combined array and the localization based classification. Although we decided to implement a combined array classification step to save computational time, directly localizing every automatically detected event is thus also possible.~~

~~The main limitation is that we could not quantify the reliability of the classifier as no independent verification data were available. Our results suggest that the HMMs trained at the Dischma array had a false alarm rate of $\sim 80\,\%$, which was reduced by applying the suggested~~ Based on the sensors used for the automatic monitoring, we identified avalanches within a range of 2 - 3 km. However, by using more sensitive sensors, e.g. seismological broadband stations, the detection range of avalanches can be increased, even up to 30 km for very large avalanches (run-out distance > 2 km (Hammer et al., 2017). However, it is difficult to deploy such sensors in mountain terrain, since these stations require existing infrastructure (e.g. electricity, storage room in a hut), which is typically not available at remote locations. In addition, the last post-processing ~~steps. However, the probability of detection or the exact false alarm rate are difficult to estimate, since ground truth data are missing.As avalanches generally release during periods of poor visibility, this is a common problem when assessing the detection performance of automatic avalanche detection systems (?Heck et al., 2018a; Thüring et al., 2015). Alternatively, one could visually inspect the waveforms and spectrograms over the entire season (e.g. van Herwijnen et al., 2016). However, events identified in this manner often contain many uncertainties (Heck et al., 2018a). For example, two of the authors independently identified possible avalanches, resulting in 44 and 23 events, respectively. Thus, the only events we could use to assess the performance of our classifier were the 13 manually identified avalanches by Heck et al. (2018b) on 9 and 10 March. Twelve of these were automatically identified with our approach, suggesting good performance in terms of probability of detection and the number of missed events~~step requires a second array. Hence low-power systems with less sensitivity proved to be the best solution. Furthermore, the limited power supply at the field sites also prevents performing first processing steps directly at the field sites

and hence limits the possibility of near real-time analysis. However, ~~we cannot make any statements on the false alarm rate, which from an operational point of view is also very important~~it is possible to overcome this problem by designing special hardware for this particular task.

Based on the approach presented here, a near real-time classification of the seismic data and hence a near real-time detection of avalanches seems possible. The computational times on a ~~standard personal computer (~~computer with a regularly available 8-core processor with 12 GB ram ~~)~~ are reasonably short ~~as feature calculation can be performed in~~ and almost near real-time ~~for all sensors simultaneously as well as the HMM construction and the classification. The MUSIC method, on the other hand,~~ whereas the localization based on the MUSIC is very costly (three times real time). ~~However, since~~ Although we decided to implement a combined array classification step to save computational time, directly localizing every detection is also possible. Since the amount of detections for the ~~entire~~ whole season was very low, a near real-time detection could be provided with or without the combined array classification. In future systems, ~~the~~ pre-processing steps can be integrated in the data logging unit to ~~substantially reduce the data transmission~~reduce the amount of data while recording. Using a standard personal computer, feature calculation is performed near real-time for all sensors simultaneously as well as the HMM construction and the classification. However, a major obstacle of our method is the necessity of an adequate training event recorded at the seismic array. Using training events recorded at different arrays might be unreliable due to possible differences in the instrumentation and changes in the overall background noise or local heterogeneities in the local geology and in snow conditions. To set up the classification experts will still be needed to define correct and confirmed training events. Future research will assess the possibility to use one training event for several seasons recorded at the same array.

6 ~~Conclusions~~

6 Conclusions

During the winter season 2016-2017 we used a seismic array to continuously monitor avalanche activity in a remote area above Davos, Switzerland. By ~~training a machine learning algorithm~~ implementing an operational classification method based on hidden Markov models (HMMs), we detected 117 events in the seismic data from January to April, which were likely produced by avalanches. Subsequent visual inspection revealed a false alarm rate of at least 50 %~~and most~~ . Most of the false detections were associated with airplanes or earthquakes. ~~We therefore trained a second HMM with data from a seismic array at a distance of 14 km to remove any co-detections. Finally, we applied a multiple signal classification~~ By implementing additional steps such as a combined array classification and the localization of the events based on multiple signal classifications (MUSIC)~~approach to define threshold criteria for automatic avalanche identification by considering avalanches as a moving source. Overall, this workflow resulted in 21 automatic classifications. The majority of these events occurred on 9 and 10 March 2017, in accordance with a period of high avalanche activity observed in the surroundings of Davos.~~

~~Our results show that seismic monitoring systems in combination with an automatic classifier provides great potential to identify at least the major avalanche periods. In our workflow, using an array processing method to determine the source of the seismic events was of crucial importance to reduce falsely classified events~~, we improved the classification results by reducing

the number of identified events to 27. Only using the localization to remove false detections resulted in at least 15 % of false detections yet at a higher computational cost. Our results therefore show that dismissing false detections with a second array improves the overall classification accuracy. If a second avalanche monitoring array is in the vicinity, combing the results of both arrays will improve the classification results. In future experiments we want to ~~introduce an additional array within a shorter distance~~ reduce the distance between the arrays to some kilometers to improve the localization ~~and no longer require the combined array classification approach~~of avalanches.

Acknowledgements. M.H. was supported by a grant of the Swiss National Science Foundation (200021_149329). We thank numerous colleagues from SLF for help with field work and maintaining the instrumentation.

Competing interests. The authors declare that they have no conflict of interest.

References

Barnes, A. E.: Instantaneous spectral bandwidth and dominant frequency with applications to seismic reflection data, Geophysics, 58, 419–428, 1993.

Bessason, B., Eiriksson, G., Thorarinsson, O., Thorarinsson, A., and Einarsson, S.: Automatic detection of avalanches and debris flows by seismic methods, J. Glaciol., 53, 461–472, https://doi.org/10.3189/002214307783258468, 2007.

Beyreuther, M., Hammer, C., Wassermann, J., Ohrnberger, M., and Megies, T.: Constructing a Hidden Markov Model based earthquake detector: application to induced seismicity, Geophys. J. Int., 189, 602–610, https://doi.org/10.1111/j.1365-246X.2012.05361.x, 2012.

Dammeier, F., Moore, J. R., Hammer, C., Haslinger, F., and Loew, S.: Automatic detection of alpine rockslides in continuous seismic data using hidden Markov models, J. Geophys. Res. Earth Surf, 121, 351–371, https://doi.org/10.1002/2015JF003647, 2016.

Esposito, A. M., Giudicepietro, F., Scarpetta, S., D'Auria, L., Marinaro, M., and Martini, M.: Automatic discrimination among landslide, explosion-quake and microtremor seismic signals at Stromboli Volcano using neural networks, Bull. Seismol. Soc. Am., 96, 1230, https://doi.org/10.1785/0120050097, +http://dx.doi.org/10.1785/0120050097, 2006.

Hammer, C., Beyreuther, M., and Ohrnberger, M.: A seismic-event spotting system for Volcano fast-response systems, Bull. Seismol. Soc. Am., 102, 948–960, https://doi.org/10.1785/0120110167, 2012.

Hammer, C., Ohrnberger, M., and Fäh, D.: Classifying seismic waveforms from scratch: a case study in the alpine environment, Geophys. J. Int., 192, 425–439, 2013.

Hammer, C., Fäh, D., and Ohrnberger, M.: Automatic detection of wet-snow avalanche seismic signals, Nat. Hazards, 86, 601–618, https://doi.org/10.1007/s11069-016-2707-0, 2017.

Heck, M., Hammer, C., van Herwijnen, A., Schweizer, J., and Fäh, D.: Automatic detection of snow avalanches in continuous seismic data using hidden Markov models, Nat. Hazards Earth Syst. Sci., 18, 383–396, https://doi.org/10.5194/nhess-18-383-2018, 2018a.

Heck, M., Hobiger, M., van Herwijnen, A., Schweizer, J., and Fäh, D.: Localization of seismic events produced by avalanches using multiple signal classifications, Geophys. J. Int., https://doi.org/10.1093/gji/ggy394, http://dx.doi.org/10.1093/gji/ggy394, 2018b.

Hibert, C., Mangeney, A., Grandjean, G., Baillard, C., Rivet, D., Shapiro, N. M., Satriano, C., Maggi, A., Boissier, P., Ferrazzini, V., and Crawford, W.: Automated identification, location, and volume estimation of rockfalls at Piton de la Fournaise volcano, Journal of Geophysical Research: Earth Surface, 119, 1082–1105, https://doi.org/10.1002/2013JF002970, https://agupubs.onlinelibrary.wiley.com/doi/abs/10.1002/2013JF002970, 2014.

Hobiger, M., Cornou, C., Bard, P.-Y., Le Bihan, N., and Imperatori, W.: Analysis of seismic waves crossing the Santa Clara Valley using the three-component MUSIQUE array algorithm, Geophys. J. Int., 207, 439–456, 2016.

Joswig, M.: Knowledge-Based Seismogram Processing by Mental Images, IEEE Trans. Syst. Man. Cybern., 24, 429 – 439, 1994.

Kanasewich, E. R.: Time Sequence Analysis in Geophysics, The University of Alberta Press, Edmonton, Alberta, Canada, 1981.

Kramer, S.: Geotechnical Earthquake Engineering, Always learning, Prentice-Hall international series in Civil Engineering and engineering mechanics, Upper Saddle River, New Jersey, 1996.

Lacroix, P., Grasso, J.-R., Roulle, J., Giraud, G., Goetz, D., Morin, S., and Helmstetter, A.: Monitoring of snow avalanches using a seismic array: Location, speed estimation, and relationships to meteorological variables, J. Geophys. Res. Earth Surf, 117, F01 034, https://doi.org/10.1029/2011JF002106, 2012.

Leprettre, B., Navarre, J., and Taillefer, A.: First results from a pre-operational system for automatic detection and recognition of seismic signals associated with avalanches, J. Glaciol., 42, 352–363, https://doi.org/10.1109/ICMLA.2012.12, 1996.

Li, Z., Meier, M.-A., Hauksson, E., Zhan, Z., and Andrews, J.: Machine Learning Seismic Wave Discrimination: Application to Earthquake Early Warning, Geophysical Research Letters, 45, 4773–4779, https://doi.org/10.1029/2018GL077870, 2018.

Marchetti, E., Ripepe, M., Ulivieri, G., and Kogelnig, A.: Infrasound array criteria for automatic detection and front velocity estimation of snow avalanches: towards a real-time early-warning system, Nat. Hazards Earth Syst. Sci., 15, 2545 – 2555, https://doi.org/10.5194/nhess-15-2545-2015, 2015.

McClung, D. and Schaerer, P. A.: The Avalanche Handbook, The Mountaineers Books, 2006.

Nishimura, K. and Izumi, K.: Seismic signals induced by snow avalanche flow, Nat. Hazards, 15, 89–100, https://doi.org/10.1023/A:1007934815584, 1997.

Ohrnberger, M.: Continuous automatic classification of seismic signals of volcanic origin at Mt. Merapi, Java, Indonesia, PhD. thesis, 2001.

Perol, T., Gharbi, M., and Denolle, M.: Convolutional neural network for earthquake detection and location, Science Advances, 4, https://doi.org/10.1126/sciadv.1700578, 2018.

Provost, F., Hibert, C., and Malet, J.-P.: Automatic classification of endogenous landslide seismicity using the Random Forest supervised classifier, Geophysical Research Letters, 44, 113–120, https://doi.org/10.1002/2016GL070709, 2016.

Rabiner, L.: A tutorial on Hidden Markov Models and selected application in speech recognition, Proceedings of the IEEE, 77, 257–286, https://doi.org/10.1109/5.18626, 1989.

Ross, Z. E., Meier, M.-A., and Hauksson, E.: P Wave Arrival Picking and First-Motion Polarity Determination With Deep Learning, Journal of Geophysical Research: Solid Earth, 123, 5120–5129, https://doi.org/10.1029/2017JB015251, 2018.

Rost, S. and Thomas, C.: Array seismology: methods and application, Rev. Geophys., 40, 2.1–2.27, https://doi.org/10.1029/2000RG000100, 2002.

Rubin, M., Camp, T., van Herwijnen, A., and Schweizer, J.: Automatically detecting avalanche events in passive seismic data, IEEE International Conference on Machine Learning and Applications, 1, 13–20, https://doi.org/10.1109/ICMLA.2012.12, 2012.

Schaerer, P. A. and Salway, A. A.: Seismic and impact-pressure monitoring of flowing avalanches, J. Glaciol., 26, 179–187, https://doi.org/10.1017/S0022143000010716, 1980.

Schmidt, R.: Multiple emitter location and signal parameter estimation, IEEE Trans. Antennas Propag., 34, 276–280, https://doi.org/10.1109/TAP.1986.1143830, 1986.

Scott, E., Hayward, C., Kubichek, R., Hamann, J., Pierre, J., Comey, B., and Mendenhall, T.: Single and multiple sensor identification of avalanche-generated infrasound, Cold Reg. Sci. Technol., 47, 159–170, https://doi.org/10.1016/j.coldregions.2006.08.005, 2007.

Steinkogler, W., Meier, L., Langeland, S., and Wyssen, S.: Operational radar and infrasound systems for avalanche detection, in: Proc. 2016 Int. Snow Sci. Workshop, Breckenridge, Colorado, USA, 3 - 7 October 2016, pp. 309–315, 2016.

Suriñach, E., Furdada, G., Sabot, F., Biescas, B., and Vilaplana, J.: On the characterization of seismic signals generated by snow avalanches for monitoring purposes, Ann. Glaciol., 32, 268–274, https://doi.org/10.3189/172756401781819634, 2001.

Suriñach, E., Vilajosana, I., Khazaradze, G., Biescas, B., Furdada, G., and Vilaplana, J.: Seismic detection and characterization of landslides and other mass movements, Nat. Hazards Earth Syst. Sci., 5, 791–798, https://doi.org/10.5194/nhess-5-791-2005, 2005.

Taner, M. T., Koehler, F., and Sheriff, R.: Complex seismic trace analysis, Geophysics, 44, 1041–1063, 1979.

Thüring, T., Schoch, M., van Herwijnen, A., and Schweizer, J.: Robust snow avalanche detection using supervised machine learning with infrasonic sensor arrays, Cold Reg. Sci. Tech., 111, 60 – 66, https://doi.org/10.1016/j.coldregions.2014.12.014, 2015.

van Herwijnen, A. and Schweizer, J.: Seismic sensor array for monitoring an avalanche start zone: design, deployment and preliminary results, J. Glaciol., 57, 257–264, https://doi.org/10.3189/002214311796405933, 2011a.

van Herwijnen, A. and Schweizer, J.: Monitoring avalanche activity using a seismic sensor, Cold Reg. Sci. Tech., 69, 165–176, https://doi.org/10.1016/j.coldregions.2011.06.008, 2011b.

van Herwijnen, A., Heck, M., and Schweizer, J.: Forecasting snow avalanches by using highly resolved avalanche activity data obtained through seismic monitoring, Cold Reg. Sci. Tech., 132, 68–80, https://doi.org/10.1016/j.coldregions.2016.09.014, 2016.